



HAL
open science

Standardization procedure to provide a unified multi-method elemental compositional dataset, application to ferruginous colouring matters from Namibia

Guilhem Mauran, Benoît Caron, Lucile Beck, Florent Détroit, Camille Noûs, Olivier Tombret, David Pleurdeau, Jean-Jacques Bahain, Matthieu Lebon

► To cite this version:

Guilhem Mauran, Benoît Caron, Lucile Beck, Florent Détroit, Camille Noûs, et al.. Standardization procedure to provide a unified multi-method elemental compositional dataset, application to ferruginous colouring matters from Namibia. *Journal of Archaeological Science: Reports*, 2022, 43, pp.103454. 10.1016/j.jasrep.2022.103454 . insu-03656248

HAL Id: insu-03656248

<https://insu.hal.science/insu-03656248v1>

Submitted on 22 Jul 2024

HAL is a multi-disciplinary open access archive for the deposit and dissemination of scientific research documents, whether they are published or not. The documents may come from teaching and research institutions in France or abroad, or from public or private research centers.

L'archive ouverte pluridisciplinaire **HAL**, est destinée au dépôt et à la diffusion de documents scientifiques de niveau recherche, publiés ou non, émanant des établissements d'enseignement et de recherche français ou étrangers, des laboratoires publics ou privés.



Distributed under a Creative Commons Attribution - NonCommercial 4.0 International License

1 Standardization procedure to provide a unified multi- 2 method elemental compositional dataset, application 3 to ferruginous colouring matters from Namibia

4 5 **AUTHORS**

6 Guilhem MAURAN^{a, b} (<https://orcid.org/0000-0002-3884-5194>),

7 Benoit CARON^c (<https://orcid.org/0000-0001-7051-4339>),

8 Lucile BECK^d,

9 Florent DÉTROIT^a (<https://orcid.org/0000-0001-5208-6203>),

10 Camille NOÛS^{e, 1}, (<https://orcid.org/0000-0002-0778-8115>),

11 Olivier TOMBRET^a,

12 David PLEURDEAU^a,

13 Jean-Jacques BAHAIN^a (<https://orcid.org/0000-0002-1446-5568>),

14 Matthieu LEBON^a (<https://orcid.org/0000-0003-4970-1230>)

15 ^a*UMR 7194 Histoire Naturelle de l'Homme Préhistorique (HNHP), Museum national*
16 *d'Histoire naturelle - CNRS -UPVD, Association Sorbonne Universités, Musée de l'Homme,*
17 *17 Place du Trocadéro, 75116 Paris, France*

18 ^b*Evolutionary Studies Institute (ESI), University of the Witwatersrand, PO Wits 2050,*
19 *Johannesburg, South Africa*

20 ^c*UMR 7193 Institut des Sciences de la Terre de Paris (ISTeP), Sorbonne Université, CNRS-*
21 *INSU, F-75005 Paris, France*

22 ^d*Laboratoire de Mesure du Carbone 14 (LMC14), LSCE/IPSL, CEA-CNRS-UVSQ, Université*
23 *Paris-Saclay, F-91191 Gif-sur-Yvette, France*

24 ^e*Cogitamus Laboratory, 1 ¾ rue Descartes, 75005 Paris, France*

25

26 Corresponding author: Guilhem MAURAN: guilhem.mauran1@edu.mnhn.fr, 0027647075419, 1 Jan Smuts
27 Avenue, Braamfontein 2000, Johannesburg, South Africa

28

29

¹ Camille Noûs embodies the collegial nature of our work, as a reminder that science proceeds from disputatio and that the building and dissemination of knowledge are intrinsically selfless, collaborative and open.

30 **ABSTRACT**

31 Curation of archaeological materials often leads to carrying out multi-analytical methodologies that
32 combine non-invasive and invasive elemental analyses. Such materials are often analysed with different
33 techniques. It results in the production of complementary but apparently non-compatible compositional
34 datasets that cannot be easily compared. In the present paper, we propose to compare results acquired
35 on geological ferruginous colouring matters from Namibia with analytical techniques (X-Ray
36 Fluorescence spectrometry (XRF), Proton-Induced-X-ray Emission spectrometry (PIXE), Inductively
37 Coupled Plasma coupled to Optical Emission spectrometry (ICP-OES) and Inductively Coupled Plasma
38 coupled to Mass Spectrometry (ICP-MS)). We aim to provide a unified elemental dataset about these
39 ferruginous colouring matters, usually referred to as “ochre” in archaeology. Analysed geological
40 samples come from three distinct tectonostratigraphic zones of Namibia surveyed in the frame of rock
41 art research. When compared directly, three of the four datasets obtained from these measurements
42 appear as non-compatible because of the inter-equipment variability. However, through a simple
43 standardization procedure, we demonstrate that it is possible to unify these datasets. This procedure
44 minimizes the inter-equipment variability, making the inter-zones of provenance predominant and
45 allowing distinctions of the samples according to their sole origin. Beyond shedding new light on the
46 possibility to compare different elemental analytical techniques, this procedure paves the way for robust
47 statistical provenance studies of ferruginous colouring matter.

48 **KEYWORDS**

49 Compositional data; Standardization; multi-method; Ferruginous colouring matter; Namibia

50

51

52

53

54

55 1.INTRODUCTION

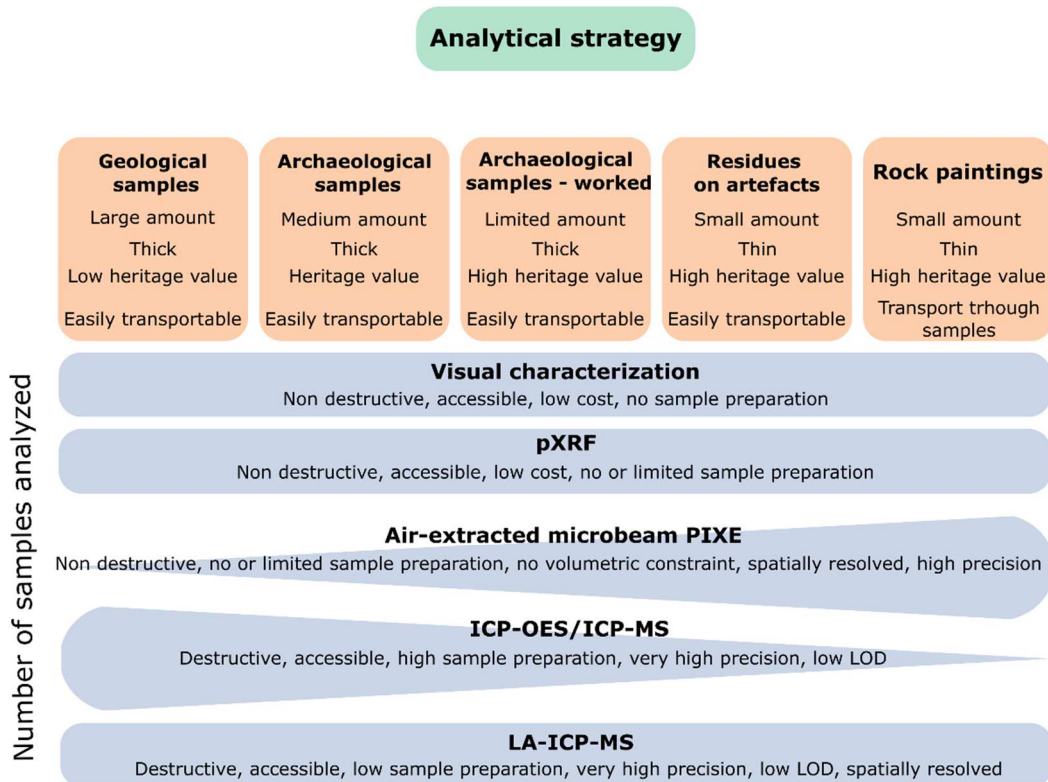
56 Ferruginous colouring matters correspond to a wide variety of rocks rich in iron-oxides which can
57 transmit their colour to another material. Most archaeologists refer to them under the “ochre” catch-
58 them-all term (Onoratini, 1985; Dayet, 2012; Chalmin et al., 2021; Salomon et al., 2021; Popelka-Filcoff
59 and Zipkin, 2022). These colouring matters occur in different archaeological contexts such as mine and
60 open-air site, rock shelter or cave. Within these contexts, they are present in various forms: as small
61 boulders and fragments in the archaeological assemblage, as residues over tools or beads or as pigments
62 used for rock art. These remains record numerous information concerning past communities cognition,
63 behaviours, techniques and mobility (d’Errico, 2003 ; Salomon et al., 2012 ; Hodgskiss, 2014; Mathis
64 et al., 2014 ; Lebon et al., 2019 ; Dayet, 2021; Domingo and Chieli, 2021; Huntley, 2021; Popelka-
65 Filcoff and Zipkin, 2022). The observation and characterization of these materials allow the description
66 of the succession of mental steps and technical gestures aimed at exploiting, processing, and using these
67 materials. This succession of steps is referred to as “*chaîne opératoire*” (Perles, 1987: 23). Here, it
68 becomes possible to investigate the methods of preparation of these resources (Wadley, 2005a,
69 Hodgskiss, 2010), the choice made by the populations in the type of colouring matter they
70 exploited (Mathis et al., 2014), their different use of these raw materials (Wadley, 2005a,b, Rifkin, 2015
71 ; Rifkin et al., 2015) , as well as the mobility of these past communities (Mauran et al., 2021a ; Huntlet,
72 2021 ; Velliky et al., 2021).

73 During the last two decades, advances in analytical instrumentation have led to an increase in the number
74 of studies about archaeological ferruginous colouring matters. These advances implied the use of
75 different elemental analytical techniques to characterize the materials and determine the provenance of
76 the archaeological ferruginous colouring matters: X-Ray Fluorescence spectrometry (XRF) (Jercher et
77 al., 1998 ; Lebon et al., 2019) , particle-induced X-ray emission (PIXE) (Erlandsen et al. 1999;
78 Bernatchez et al. 2008 ; Nel et al., 2010 ; Beck et al., 2011. 2012 ; Salomon et al., 2012 ; Mathis et al.,
79 2014 ; Lebon et al., 2014) , instrumental neutron activation analysis (NAA) (Kiehn et al., 2007 ;
80 Popelka-Filcoff et al., 2007, 2008 ; Eiselt et al., 2011 ; MacDonald et al., 2013, 2018 ; Velliky et al.,
81 2021) , inductive coupled plasma – optical emission spectrometry and mass spectrometry (ICP-OES
82 and ICP-MS) coupled or not to laser ablation (Green an Watling, 2007 ; Iriarte et al., 2009 ; Dayet et
83 al., 2013 ; Scadding et al., 2015 ; Moyo et al., 2016 ; Zipkin et al., 2017, 2020 ; Eiselt et al., 2019 ;
84 Pierce et al., 2020 ; Mauran et al., 2021a) . An extensive review of these studies has been recently
85 published by Dayet (2021) .

86 The aforementioned techniques present different advantages and disadvantages regarding their
87 analytical specificities: destructiveness, analytical costs, range of measured elements at once,
88 repeatability and accessibility (Fig. 1). There is a clear demand for instruments with high repeatability
89 and accuracy but also economical, widely accessible and of minimal invasiveness for preserving these

90 unique archaeological artefacts. Not all these requirements can be met altogether, often leading
 91 researchers to downscale their studies and repeat analyses of the same sample with different analytical
 92 techniques. The selection of one of these techniques is material, context, and problem dependant
 93 (Salomon et al., 2016 ; Zipkin et al., 2020 ; Dayet, 2021) . The development of multi-technical
 94 approaches, combining non-invasive and invasive analyses allow accessing all different aspect of past
 95 exploitations of ferruginous colouring matter (Dayet , 2012 ; Chalmin and Huntley, 2018 ; Mauran, 2019
 96 ; Domingo and Chieli, 2021).

97 When one tries to study the whole “*chaîne opératoire*” of these ferruginous resources, the absolute
 98 necessity of their preservation leads to carrying out multi-analytical methodologies that combine non-
 99 invasive and invasive analyses. On one side, using ICP-OES/ICP-MS on geological samples would
 100 provide an accurate fingerprint of the potential sources, but result in destroying the samples, which can’t
 101 be done for most of archaeological assemblages On the other side, using non-destructive but less
 102 sensitive analyses such as air-extracted microbeam PIXE and pXRF for highly valued archaeological
 103 samples and residues would allow their preservation while providing limited information about their
 104 potential provenance (Fig. 1) (Mauran, 2019) .



105

106 Fig. 1. Ideal analytical strategy to investigate the geochemical composition of ferruginous colouring
 107 matter. (double columns, colour)

108 The use of these techniques with different sensitivity and precision produces complementary but non-
109 compatible compositional datasets. However, between-laboratory variations can limit comparisons of
110 datasets acquired from distinct instruments or even on different days (Yellin et al., 1978 ; Popelka-
111 Filcoff et al., 2012 ; Salomon et al., 2016) Fundamental differences in experimental conditions between
112 distinct techniques raise more difficulties (Hein et al., 2002 ; Tsolakidou et al., 2002 ; Glascock et al.,
113 2004) . So far, this has prevented researchers to reuse and share compositional data of ferruginous
114 colouring matter acquired with different techniques or at distinct laboratories thus restricting studies to
115 answer punctual questions (Salomon et al., 2016 ; Chanteraud et al., 2021). Previous works attempted
116 to compare data acquired on ferruginous colouring matter samples with different techniques (SEM-EDS,
117 PIXE, ICP-OES) (Dayet, 2012, 2021). Dayet mainly investigated the accuracy of these techniques and
118 highlighted the influence of patina on geochemical data. Works performed by Salomon and colleagues
119 (2016) shed light on the importance of using standards to compare data. Popelka-Filcoff and colleagues
120 (2012), compared NAA measures acquired at two different facilities. They concluded to the equivalence
121 of the datasets but the impossibility to combine them directly. Research aiming to compare data acquired
122 by different analytical methods have been carried out on other materials such as ceramics, glaze, and
123 obsidians (Hein et al., 2002 ; Grave et al., 2005 ; Speakman et al., 2011 ; Mitchell et al., 2012 ;
124 Kasztovszky et al., 2018). However, all these works only compared the techniques and their efficiency
125 to discriminate the provenance origins of different raw material. Inter-equipment calibrations remain
126 scarce, one of the most successful projects is the CHARM project. During this project, Heginbotham
127 and colleagues (2015) have developed XRF inter-laboratory standardization for copper alloys
128 characterization. Maximum Fe_2O_3 content in these alloys is of $1.4 \pm 0.9 \%$ (32X SN5A) (Heginbotham
129 et al., 2015 ; Steenstra et al., 2021). Ferruginous colouring materials usually have a Fe_2O_3 content
130 comprised between 10 to 90 %. This difference of composition prevents the direct use of this inter-
131 laboratory calibration for colouring materials characterization. Elemental analyses provide large datasets
132 usually containing more than ten elemental concentrations (variables) and often a higher number of
133 samples (observations). Questions answered with these elemental analyses usually consist in 1)
134 discriminating groups of artefacts according to their elemental composition (categorisation), 2)
135 comparing the artefacts elemental composition with modern raw material elemental composition
136 (sourcing). Answering these questions involves investigating the structure of the elemental datasets. To
137 do so, researchers often use exploratory multivariate analyses. Among the most often used multivariate
138 analyses are principal component analysis (PCA) and linear discriminant analysis (LDA). Both analyses
139 are presented in detail for ochre studies by Zipkin and colleagues (2017), and iron slags by Leroy (2010)
140 or more generally by Baxter (1994) .

141 Principal component analysis (PCA) is most of the time used as an unsupervised method.... PCA allows
142 reduction of the number of variables and mainly maximises the variability over the whole dataset. Linear
143 discriminant analysis (LDA) is a supervised method that also allows reducing the number of variables

144 but maximises the ratio of between-class variance to within-class variance. In this sense, LDA is more
145 susceptible to discriminate groups than PCA, due to the inherent structure provided to perform the
146 analysis. In this sense, PCA allows the investigation of the structure of the datasets while LDA allows
147 better discrimination of distinct groups.

148 PCA, the most common method used in colouring matter provenance, is a scale dependant analysis.
149 Therefore, variables with the highest intensity weigh more than others in the statistical analysis. When
150 investigating datasets with concentrations expressed in different units such as percentages and parts per
151 million, data treatments are a necessity to ensure an equal weight to all the variables. This is why data
152 are usually transformed. Numerous transformations exist to tackle this issue. Data standardization to
153 zero mean and unit variance or log-ratio transformations are however the most common, sometimes
154 used together (Baxter, 1995) .

155 The use and advantages of standardization and log-transformation have been debated elsewhere
156 (MacDonald et al., 2013, 2018 ; Zipkin et al., 2017, 2020 ; Mauran et al., 2021a) . The most common
157 method for colouring matter provenance studies relies on the Fe- normalization methodology (e.g. David
158 et al., 1993 ; Smith et al., 1998 ; Popelka-Filcoff et al., 2007). After a statistical correlation test such as
159 Pearson's is performed, only elements correlated with Fe are used in subsequent analyses.
160 Considerations about elements correlation are further discussed in the literature (e.g. Popelka-Filcoff et
161 al., 2007; Beck et al., 2011; Mathis et al., 2014; Lebon et al., 2018; MacDonald et al. 2011; Dayet et al.,
162 2016; Dayet, 2021). These elements are then normalized to the iron content. These ratios are then log-
163 transformed. But recent studies have highlighted some of the limits of this method (Dayet et al., 2016 ;
164 MacDonald et al., 2018, Pierce et al., 2020) Other transformations such as direct logarithm or centred-
165 log-ratio transformations have been successfully developed (Zipkin et al., 2017 ; Pierce et al., 2020;
166 Mauran et al., 2021a) . The centred-log-ratio transformation is a more general transformation than the
167 Fe-log-ratio one, for which elemental concentrations are normalized to the geometrical mean of the
168 concentrations of all elements considered. According to Aitchison (1982), this transformation is more
169 robust than the Fe-log-ratio transformation to sub-composition (a subset composition) use.

170 Since 2015, we investigate the use of ferruginous colouring matters at the Later Stone Age site of
171 Leopard Cave (Erongo, Namibia) (Mauran et al., 2020, 2021a,b). A large part of the colouring matters
172 recovered at the site are massive haematites. We already proved the possibility to provenance Namibian
173 ferruginous colouring matter with invasive ICP-OES/ICP-MS technique (Mauran et l., 2021a) . But such
174 a procedure is only possible for geological and few unmodified archaeological blocks leaving aside most
175 of the archaeological artefacts. Therefore, most of the "*chaîne opératoire*" remains difficult to
176 investigate. As we aim to study the whole "*chaîne opératoire*" of ferruginous colouring matter

177 processing, we investigated the possibility to compare compositional data acquired with different
178 analytical techniques. We hope to combine their advantages as presented in figure 1.

179 In this paper, we apply multivariate analysis on datasets obtained on colouring materials from central
180 Namibia by X-Ray Fluorescence spectrometry (XRF), Proton-Induced-X-ray Emission spectrometry
181 (PIXE), Inductively Coupled Plasma coupled to Optical Emission spectrometry (ICP-OES) and
182 Inductively Coupled Plasma coupled to Mass Spectrometry (ICP-MS). We aim to unify these different
183 compositional datasets of ferruginous colouring matters to provide the possibility to study the whole
184 “*chaînes opératoires*” and have a better understanding of past populations behaviours and mobility. Our
185 results are relevant beyond the scope of ferruginous colouring materials as they can provide a way to go
186 for multimodal inter laboratory comparisons of artefacts of high cultural heritage importance, which
187 cannot be analysed destructively.

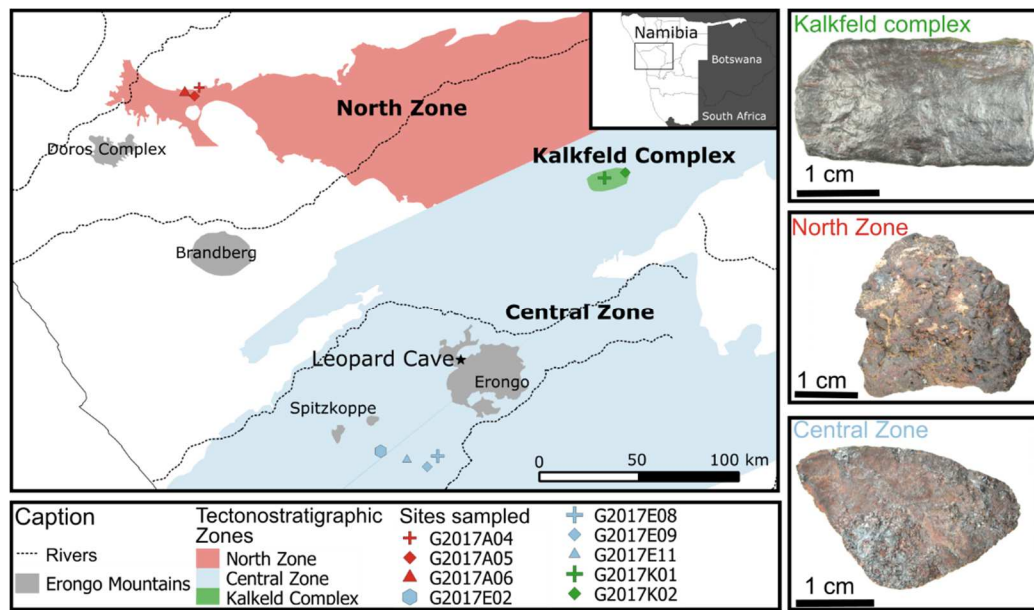
188 **2.MATERIAL AND METHODS**

189 **2.a. Material**

190 Ferruginous colouring matters analysed in this study are geological samples. We collected them at seven
191 outcrops in three distinct tectonostratigraphic zones around Leopard Cave in north-central Namibia
192 (Mauran et al., 2021a, b). These three zones are the North Zone (NZ), the igneous Kalkfeld Complex
193 (Kalkfeld), and the Central Zone (CZ) (Fig. 2). They respectively correspond to what we previously
194 considered as regional provenance, sub-local provenance and local provenance areas (Mauran et al.,
195 2021a). Our initial archaeological question focused on the existence of raw material circulation between
196 different Namibian rock art massif. Each of the massif falls into different tectonostratigraphic zone
197 (Mauran et al., 2021a). This is why, we grouped different localities into groups corresponding to the
198 tectonostratigraphic zones. All samples were collected in 2017 and exported in agreement with permit
199 ES 31957 granted to G.M. Table 1 sums up the origin and the analyses performed on each sample. 52
200 samples were analysed by XRF, 23 by PIXE and 55 by-both-ICP-OES and ICP-MS by a same operator
201 with the help of specialists of each analytical method. Samples from Kalkeld zone correspond to igneous
202 hematite-magnetite ore and ferruginous breccia form from their alteration. Samples from the North Zone
203 correspond to hematite -goethite nodules of volcanic and igneous origin and hematite sandstone
204 resulting from their alteration. Samples from the Central Zone are ferruginous hematite-goethite nodules
205 come from lens of possible igneous origin.

206 Standards BXN (bauxite), DRN (diorite), IFG (iron formation) from SARM Laboratory (CRPG Nancy)
207 and 11 samples were analysed with all four methods: ICP-OES, ICP-MS, PIXe and pXRF (Table 2).
208 Among these 11 samples, four came from Kalkfeld complex, 4 from Central Zone and 3 from North
209 Zone.

210



211

212 Figure 2. Geological context (left) and selected examples (right) of the Namibian geological samples
 213 analysed in the study. (double column, colour)

214

215

Outcrop	Zone	Number of samples analysed by ICP	Number of samples analysed by PIXE	Number of samples analysed by pXRF
G2017K01	Kalkfeld Complex	3	2	5
G2017K02	Kalkfeld Complex	6	2	5
Total Kalkfeld Complex		9	4	10
G2017E02	Central Zone	10	3	5
G2017E08	Central Zone	7	4	7
G2017E09	Central Zone	5	0	5
G2017E11	Central Zone	7	4	6
Total Central Zone		29	8	23
G2017A04	North Zone	5	2	5
G2017A05	North Zone	5	2	7
G2017A06	North Zone	8	4	7
Total North Zone		18	8	19
Total		56	23	52

216 Table 1. List of outcrops from which samples were analysed in this study with mention of their
217 tectonostratigraphic zone of origin.

218 **2.b. XRF analysis**

219 X-ray fluorescence spectrometry (XRF) analyses were carried out at the Musée de l'Homme, MNHN,
220 Paris, France using an Elio portable X-Ray fluorescence spectrometer developed by XGLAB (Bruker).
221 This system is composed of an X-ray source based on an Rh anode. The anode operates at a voltage
222 between 10 and 40 kV and a current up to 200 μ A for maximal power of 4 W. Detection is ensured by a
223 Silicon Drift Detector with an active area of 25 mm². The emitted beam source is collimated to a spot
224 diameter of 1.2 mm on the sample at a working distance of 1.4 cm. Analyses were performed at 40 kV
225 and 100 μ A, with an accumulation time of 300 s. Spectra were treated using PyMca software to calculate
226 elemental concentrations from fundamental parameters (Solé et al., 2007). Usually, this fundamental
227 parameters approach does not require a standard calibration. To validate our approach, we measured
228 three standards: BXN, DRN and IFG. All these samples were prepared as pressed powders. As pXRF
229 has relatively high LOD for minor and trace elements for ferruginous materials, LOD were estimated
230 and values below LOD were subjected to zero-substitution (see Data treatment). For pXRF analyses,
231 samples were analysed as is. Most samples presented “fresh” break with no patina. Samples weight
232 between 3 to 80g. Raw pXRF results are presented in Electronic Supplementary Information (ESI) 1.

233 **2.c. PIXE analysis**

234 Proton-induced X-ray Emission spectrometry analyses have been carried out with the external proton
235 beam of NEW-AGLAE (C2RMF, Louvres Museum, Paris, France) (Pichon et al., 2015 ; Lebon et al.,
236 2018) . Before analysis, samples were sawed to obtain a plan of analyses inside each sample with
237 minimal influence of the outside patina or any surface contamination. The cut samples were then
238 analysed with no further preparation. Measurements were performed using 3 MeV protons beam with a
239 diameter of around 40 μ m on samples. Large areas (at least 2 x 2 mm) were scanned thanks to
240 horizontal/vertical mechanical movements to average samples composition. Time acquisition, around 3
241 min, was adjusted according to a dose rate detector to obtain an identical dose on each sample.

242 Low and high energy X-Ray emissions were recorded using Peltier-cooled SDD detectors (50 mm²).
243 One detector was devoted to low energies (Mg to Fe) and three to high energies (Fe and above). Two
244 high energy detectors were covered by a 20 μ m thick chromium and a 50 μ m thick aluminium filter.
245 The third high energy detector was covered by a 150 μ m thick aluminium filter. These filters reduce
246 pileup effects and the X-rays induced by the Cr filter (Swann et al., 1990 ; Beck et al., 2012) . Fe
247 quantification was used as a pivot between the low and high energies (Beck et al., 2011). The selected
248 experimental conditions are similar to previous PIXE ferruginous colouring matters analyses carried out
249 at AGLAE (Beck et al., 2011, 2012 ; Lebon et al., 2018). In such conditions, the detection limits are

250 between 10 and more than 100 ppm according to the element. Spectra treatment and elemental
251 quantification were performed using TRAUPIXE and GUPIX software (Pichon et al., 2010). The
252 GUPIX software relies on the use of a configuration file that allows spectrum modelling considering the
253 specificities of each experiment. The configuration file used was optimised by measurement performed
254 on the DRN (diorite, 70% aluminosilicate) standard, used to compare PIXE day to day quantifications.
255 All three standards BXN, DRN and IFG were prepared as pressed powders. Raw PIXE results are
256 presented in ESI 2.

257 **2.d. ICP-OES and ICP-MS analysis**

258 Elemental characterization of each sample was performed using both solutions Inductively Coupled
259 Plasma Optical Emission Spectroscopy (ICP-OES) and Inductively Coupled Plasma Mass Spectrometry
260 (ICP-MS) at the ALIPP6 Platform (Sorbonne Université, IStEP). 100 mg of homogenized powder (50
261 mg for ICP-OES and 50 mg for ICP-MS) were digested in acidic solutions and then analyzed according
262 to the protocol of the ALIPP6 and published by Mauran and colleagues (Mauran et al., 2021a). In
263 addition to standards BXN, DRN, IFG, ICP-OES and ICP-MS were calibrated thanks to the following
264 reference materials: FeR-1 (Iron formation), FeR-2 (Iron formation), FeR-3 (Iron formation), FeR-4
265 (Iron formation), ATHO-G (rhyolitic glass), BHVO-2 (basalt), BCR-1 (basalt), BIR-1 (basalt), GSN,
266 and RGM-1(rhyolite) (ESI 3). All these standards were prepared according to the same protocol than
267 the samples. Raw ICP-OES and ICP-MS results are presented in ESI 4 and on the online open access
268 repository (Mauran et al., 2021b – <http://doi.org/10.5281/zenodo.3908304>).

269 ICP-OES analyses were carried out on a 5100 SVDV Agilent ICP-OES and allowed us to quantify the
270 following 21 chemical elements: Si, Al, Mg, Na, K, Ti, Fe, Mn, Ca, P, Sr, Ba, Sc, V, Cr, Zr, S, W, Cu,
271 Zn, Co. For each of these elements, between two and four wavelengths were measured over an exposure
272 time of 3 times 20 s.

273 ICP-MS analyses were carried out on a 8800 Agilent ICP-MS/MS and allowed us to quantify the
274 following 37 chemical elements: ⁷Li, ⁴⁵Sc, ⁵¹V – ⁵³V, ⁵²Cr, ⁵⁹Co, ⁶⁰Ni, ⁶³Cu, ⁶⁶Zn, ⁷¹Ga, ⁷⁵As, ⁸⁵Rb, ⁸⁸Sr,
275 ⁸⁹Y, ⁹⁰Zr, ⁹³Nb, ⁹⁵Mo, ¹³³Cs, ¹³⁷Ba, ¹³⁹La, ¹⁴⁰Ce, ¹⁴¹Pr, ¹⁴⁶Nd, ¹⁴⁷Sm, ¹⁵³Eu, ¹⁵⁷Gd, ¹⁵⁹Tb, ¹⁶³Dy, ¹⁶⁵Ho,
276 ¹⁶⁶Er, ¹⁶⁹Tm, ¹⁷²Yb, ¹⁷⁵Lu, ¹⁷⁸Hf, ¹⁸¹Ta, ²⁰⁶Pb – ²⁰⁷Pb – ²⁰⁸Pb, ²³²Th, ²³⁸U .

277 Our comparison of elements concentration quantified by ICP-OES and ICP-MS (V, Cr, Co, Cu, Zn, Sr,
278 Zr, Ba, Sc) demonstrated that the two techniques are complementary (Mauran et al., 2021a). The ICP-
279 OES analyses allow the quantification of major, minor and few trace elements, while ICP-MS ones
280 provide quantification of a large range of trace elements. To avoid elements redundancy between the
281 ICP-OES and ICP-MS measures, we arbitrary decided to use for subsequent analyses the ICP-MS values
282 for these elements (Mauran et al., 2021a).

283 2.e. Data treatment

284

285 **Zero Value substitution.** Common data treatment for ferruginous colouring matters data statistical
286 analyses rely on the use of logarithm (e.g. David et al., 1993 ; Popelka-Filcoff et al., 2007, 2008). One
287 issue of the use of logarithm is the existence of zero values. Zero values could correspond to a real
288 absence, called “essential” zero, or to the presence of an element in smaller quantities than the limit of
289 detection (LOD), called “rounded” zero. Because these “rounded” zero are different than the “essential”
290 zero it seems reasonable to replace them. In compositional studies, several approaches exist to replace
291 these zero values. Two large families of substitution procedure exist: Simple substitutions or advanced
292 substitutions procedures. Simple substitutions rely on replacing the rounded zero for a constant positive
293 value smaller than the limit of detection of the analytical technique used to perform the measurement
294 (Palarea-Albaladejo et al. 2014). As such simple approach risks biasing the datasets more advanced
295 substitution have been developed (Aitchison, 1986 ; Baxter, 1994 ; Martín-Fernández et al. 2003 ;
296 Palarea-Albaladejo and Martín-Fernández 2013). These advanced methods attempt to preserve the ratio
297 relationship among the variables (or in our case element) thanks to closure procedure. However, closing
298 the data to 100 % can induce false elemental correlation and that only the ratio between the elements is
299 of interest for compositional data analyses (Aitchison, 1982). In ochre studies, rounded zero substitution
300 has been discussed by Zipkin et al., (2020)

301 As we decided to avoid closure procedures for the reasons mentioned above, in the current study, we
302 decided to perform a “simple substitution”. Before applying logarithm transformation, concentrations
303 below the limits of detection of the considered technique were substituted by a value of 10% of the
304 minimal value.

305 **Standardization procedures.** To unify the obtained datasets, two different standardization procedures
306 were tested in the present study. The two procedures only differ in the way we performed the merger
307 and standardization of the dataset obtained from the different analytical technique. Both standardization
308 procedures relied on the following formula:

$$309 \quad x_{ij} = \frac{C_{ij} - \bar{C}_i}{\sigma C_i} \quad (1)$$

310 where x_{ij} is the standardized concentration of an element i for a sample j , C_{ij} the concentration of an
311 element i for a sample j , \bar{C}_i the mean concentration of element i in all samples, and σC_i the standard
312 deviation of element i concentration.

313 The first procedure referred to post merged standardization consisted in applying formula (1) on the
314 merged datasets without any consideration of the analytical techniques providing the measure. The
315 dataset obtained from this first procedure is called the post merged dataset (ESI 5).

316 The second standardization procedure consisted in applying formula (1) on each dataset separately
317 before merging the datasets. We refer to the connected transformed dataset as the pre merged dataset
318 (ESI 6).

319 **Statistical analyses.** All statistical analyses were performed with the R software version 3.6.2 and the
320 “ggplot2”, “ade4”, “MASS”, “corrplot”, “MVN” packages (Chessel et al., 2004 ; Wickham, 2011;
321 Ripley et al., 2013 ; Korkmaz et al., 2014 ; Wei et al., 2017) . Used scripts are provided in supplementary
322 data (ESI 7).

323 We tested the multivariate normality of our raw data with the Mardia’s multivariate skewness and
324 kurtosis test, Royston’s multivariate Shapiro–Wilk test and the Henzee Zirkler empirical characteristic
325 function test using the MVN statistical package for the R programming environment (Korkmaz et al.,
326 2014 ; Cain et al., 2017) . All three MVN tests found that our data sets are non-multivariate normal. As
327 LDA has been considered as robust to violations of data set multivariate normality, we pursued our
328 analysis (Blanca et al., 2013 ; Enserro et al., 2019). The use of logarithm scaling decreases the existing
329 bias due to the difference of scale of concentration between the distinct elements under consideration
330 (Baxter, 1994 ; MacDonald et al., 2018). For ochre sourcing studies as ours, such a transformation is
331 essential, given the difference of magnitude between the major, minor and trace elements. Moreover,
332 the log transformation allows the reduction of the multivariate non-normality of the measures
333 distribution and increases the robustness of the statistical performance (Buxeda i Garrigós, 2018) .

334 After these treatments we used Principal Components Analysis (PCA) and Linear Discriminant Analysis
335 (LDA). To evaluate the performance of LDA on the different datasets considered, we performed cross-
336 validation tests. The cross-validation tests were based on calculation of the confusion matrix using the
337 confusion function published by Maindonald and Braun (2006) . It is calculated from predictions of
338 class membership that are derived from leave-one-out cross-validation and comparison of the actual
339 given and predicted group assignments.

340 **3.RESULTS**

341 **3.a. Standards and techniques performances**

342 **Major elements.** Raw concentrations measured on the DRN, BXN and IFG standards are presented in
343 Table 2.

<i>Standard</i>	<i>Analytical technique</i>	<i>Na₂O</i>	<i>MgO</i>	<i>Al₂O₃</i>	<i>SiO₂</i>	<i>CaO</i>	<i>K₂O</i>	<i>TiO₂</i>	<i>Fe₂O₃</i>
<i>BXN</i>	Certified	0.1	0.1	54.2 ± 1.2	7.4 ± 0.5	0.2 ± 0.1	<0.1*	2.4 ± 0.2	23.2 ± 0.8
	ICP (OES)	<0.1*	0.1 *	61.7 ± 0.2	8.2 ± 0.1	0.3 ± 0.1	<0.1	2.6*	26.8 ± 0.1
	PIXE	<LOD	0.3 ± 0.1	60.8 ± 1.1	9.6 ± 0.3	0.3 ± 0.2	<0.1*	2.7 ± 0.1	25.5 ± 0.6
	pXRF	NM	NM	47.9 ± 1.6	7.1 ± 0.1	0.2 *	<0.1*	2.4 ± 0.1	24.3 ± 1.0
<i>DRN</i>	Certified	3	4.4	17.5 ± 0.6	52.9 ± 0.7	7.1 ± 0.2	1.7 ± 0.1	1.1 ± 0.1	9.7 ± 0.3
	ICP (OES)	3*	4.4*	17.8 ± 0.1	54.1 ± 0.3	7.1*	1.7 ± 0.2	1.1 *	9.7*
	PIXE	3 ± 0.1	4.2 ± 0.2	17.7 ± 0.3	52.9 ± 0.8	6.9 ± 0.2	1.7**	1.1 ± 0.1	10.0 ± 0.5
	pXRF	NM	NM	21.2 ± 9.8	56.9 ± 15.0	7.0 ± 1.1	1.9 ± 0.3	1.0 ± 0.1	11.8 ± 1.4
<i>IFG</i>	Certified	<0.1**	1.8 ± 0.2	0.2 ± 0.1	41.2 ± 0.7	1.6 ± 0.2	<0.1*	<0.1*	55.9 ± 0.1
	ICP (OES)	<0.1**	1,8**	0.2*	40.4 ± 0.2	1.4*	<0.1*	<0.1*	55.7 ± 0.1
	PIXE	0.4 ± 0.2	2.2 ± 0.2	0.3*	39.0 ± 0.7	1.5 ± 0.1	<0.1*	<0.1*	55.0 ± 0.7
	pXRF	NM	NM	3.2 ± 0.5	43.7 ± 8.6	1.9 ± 0.1	<0.1*	<0.1*	53.8 ± 3.2

345 Table 2. Certified and mean measured concentrations of major and minor elements for the DRN, BXN and IFG standards (% wtO). (NM: non measured, LOD:
346 Limit of Detection, * standard deviation not provided by reference material certificate, ** standard deviation < 0,1 %).

347 For ICP-OES, most standard deviations are low, often below 0,01 % (Table 2), thanks to the good
348 repeatability of the technique. Most ICP-OES measures fall within the incertitude range of the certified
349 values. Discrepancies are observed for major elements (Al_2O_3 , SiO_2 , Fe_2O_3) for standard BXN, a
350 standard with a loss of ignition of 11.5 %. LOI for DRN and IFG are 2.2 and -1.1% respectively. Thus,
351 the discrepancies could be related to the high LOI of the BXN.

352 PIXE concentrations present similar accuracy and discrepancies that seems related to the LOI (Table 2).
353 Configuration parameters used for concentration computation using GUPIX software were tested on
354 samples with low LOI, including DRN. Measurements of a sample with a higher LOI as BXN do not
355 appear accurate (Table 2).

356 pXRF results are close to the certified values and fall within their incertitude range. They present higher
357 discrepancies with the certified concentrations than PIXE and ICP-OES ones (Table 2). Major
358 discrepancies exist for all three standards for Al_2O_3 content. This is imputable to the low weight of the
359 element and the existence of some overlapping with L and M bands of heavier elements. Though the
360 measures acquired the three techniques are of the same estimate, possibly allowing their comparison.

361 **Trace elements.**

362 Most trace elements (As, Ba, Cu, Cr, Ga, Mn, Ni, Pb, Rb, Sr, V, W, Y, Zn) confirm the previous results:
363 good accuracy and repeatability of PIXE and ICP-OES and lower accuracy and repeatability for pXRF
364 (Table 3). Most measures fall within the range of uncertainty of the certified values. LOD of PIXE and
365 pXRF non-destructive are higher than the ones of ICP-MS and ICP-OES for most elements (Table 3).
366 The high LOD of PIXE for Cr is due to the use of a Cr filter. Sulphur concentrations appeared highly
367 inaccurate and unprecise for all the techniques used in our study. Therefore, we did not consider this
368 element in our following analyses.

369 Contrary to Chanteraud et al. (2021), who did not calibrate their pXRF, unifying the data sets seems
370 possible. Therefore, we decided to investigate the possibility to unify these different measures despite
371 the existing discrepancies.

Standard	Analytical technique	As	Ba	Cu	Cr	Ga	Mn	Ni	Pb	Rb	Sr	V	W	Y	Zn	Zr	S
BXN	Certified	115 ± 9	30 ± 7	18 *	280 ± 75	67 ± 19	387 ± 155	180 ± 37	135 ± 77	3 ± 11	110 ± 19	350 ± 77	9 *	114 ± 40	80 ± 39	590 ± 86	NM
	ICP-MS	115 ± 7	24 ± 3	19 ± 1	270 ± 1	67 ± 5	NM	175 ± 10	153 ± 28	4 ± 1	110 ± 4	343 ± 2	NM	94 ± 2	77 ± 4	298 ± 3	NM
	ICP-OES	NM	41 ± 5	10 ± 2	268 ± 5	NM	509 ± 5	NM	NM	NM	109 **	355 ± 3	<LOD	NM	86 ± 5	329 ± 13	372 ± 249
	PIXE	130 ± 8	<LOD	14 ± 3	<LOD	70 ± 5	384 ± 31	204 ± 18	163 ± 13	2 ± 4	124 ± 6	462 ± 79	<LOD	112 ± 5	87 ± 8	567 ± 96	1414 ± 1787
	pXRF	174 ± 71	<LOD	<LOD	328 ± 18	46 ± 2	522 ± 122	218 ± 14	146 ± 14	6 ± 5	72 ± 7	348 ± 21	<LOD	61 ± 3	55 ± 3	580 ± 30	NM
DRN	Certified	3 ± 1	385	50 ± 7	40 ± 11	22 ± 5	1704 ± 155	15 ± 11	55 ± 7	73 ± 8	400 ± 50	220*	130 *	26 ± 7	145 ± 17	125 ± 25	350
	ICP-MS	3 **	368 ± 33	45 ± 3	34 ± 1	22 ± 1	NM	16 ± 1	53 ± 9	70 ± 3	386 ± 5	205 ± 2	NM	26 ± 1	134 ± 2	26 ± 1	NM
	ICP-OES	NM	375 ± 6	45 ± 1	36 ± 2	NM	1685 ± 52	NM	NM	NM	393 ± 3	208 ± 2	114 ± 7	NM	140 ± 4	24 ± 1	1048 ± 623
	PIXE	4 ± 3	300 ± 188	54 ± 7	<LOD	22 ± 3	1787 ± 103	<LOD	61 ± 9	72 ± 4	399 ± 19	219 ± 44	136 ± 8	23 ± 4	155 ± 9	99 ± 50	7044 ± 1420
	pXRF	<LOD	337 ± 180	46 ± 6	<LOD	24 ± 2	2235 ± 259	<LOD	37 ± 7	73 ± 6	427 ± 40	180 ± 34	129 ± 8	18 ± 1	156 ± 6	186 ± 16	NM
IFG	Certified	2 ± 1	2*	10 ± 3	9 ± 3	1*	325 ± 108	23 ± 16	4*	1*	3*	2*	220 ± 60***	9*	20 ± 7	1*	700*
	ICP-MS	1**	<1**	13 ± 1	9**	<1**	NM	26 ± 1	4 ± 1	1**	<1**	4**	NM	8**	20 ± 5	4**	NM
	ICP-OES	NM	11 ± 7	3 ± 2	11 ± 3	NM	318 ± 30	NM	NM	NM	3 ± 4	7 ± 5	44 ± 18	NM	45 ± 2	8 ± 1	1612 ± 925
	PIXE	6 ± 1	<LOD	10 ± 3	<LOD	<LOD	323 ± 40	<LOD	1 ± 2	<LOD	<LOD	<LOD	<LOD	8 ± 5	26 ± 2	2 ± 2	230 ± 326
	pXRF	<LOD	<LOD	<LOD	<LOD	<LOD	471 ± 217	27 ± 14	<LOD	<LOD	<LOD	<LOD	75 ± 42	<LOD	26 ± 12	<LOD	NM

372 Table 3. Certified and mean measured concentrations of trace elements for the DRN and BXN standards in ppm. (NM: non measured, LOD: Limit of
373 Detection, *standard deviation not provided by standard certificate, ** standard deviation < 1 ppm, *** existing discrepancies between literature and standard
374 certificate).

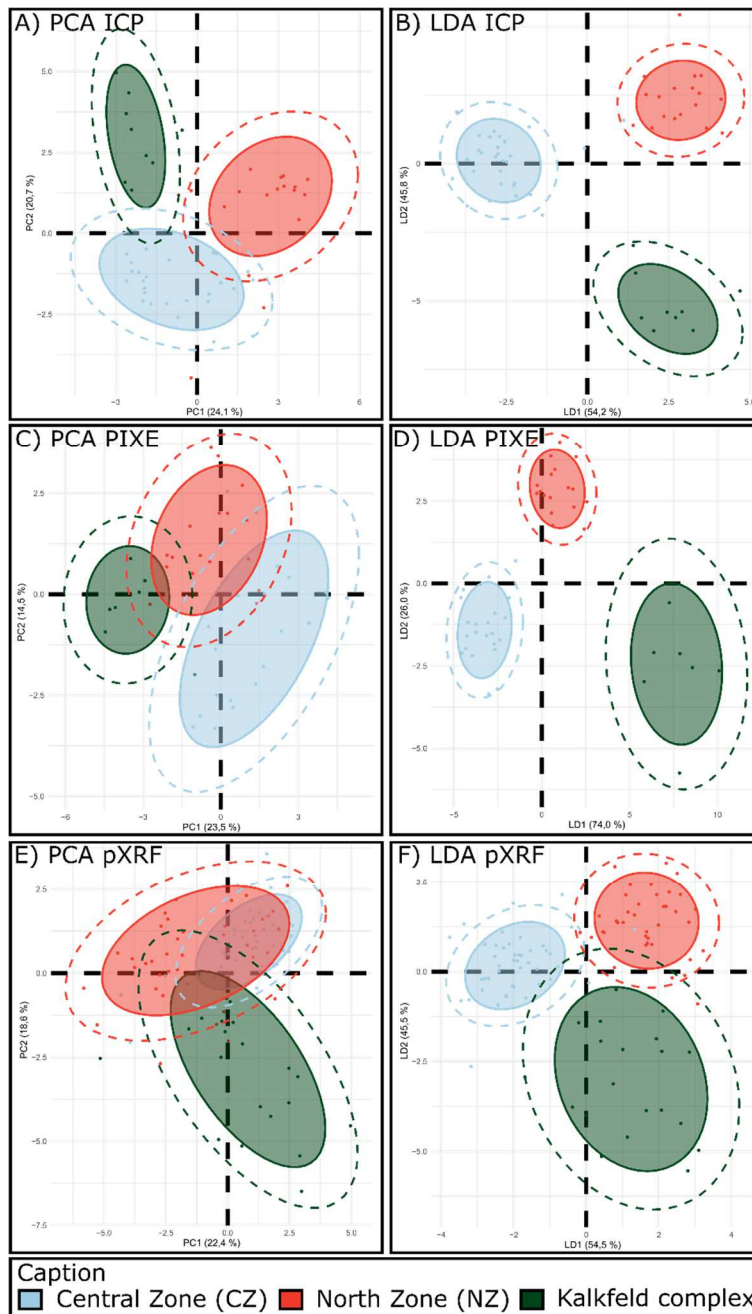
375 **3.b. ICP-OES and ICP-MS results**

376 We already demonstrated the possibility to differentiate ferruginous colouring matter from five different
377 tectonostratigraphic zones thanks to ICP-OES/ICP-MS and multivariate statistics (Mauran et al., 2021a).
378 Among the five zones discriminated in our previous study, are the three zones studied in the present
379 study.

380 For the present study, 55 samples were analysed both by ICP-OES and ICP-MS (Table 1). Raw
381 elemental concentration data are provided in ESI 4. We first aimed to confirm the possibility to
382 differentiate the three zones thanks to ICP-OES and ICP-MS data. Therefore, ICP-OES/ICP-MS
383 centred-log-ratio transformed data were submitted to principal component analysis and linear
384 discriminant analysis for the following elements: Al, Ca, Fe, K, Mn, P, Si, Ti, Cr, Ni, Zn, W, Cu, Y, As,
385 Sr, Zr, Mo, Ga, Pb.

386 Biplots of the first two principal components are plotted in Fig. 3 and component loadings are given in
387 ESI 8. For PCA (Fig 3.A), the first two components account for 44,8 % of the total variation, and are
388 mostly driven by Cu, Ni, Cr, As, Zr, Pb, Ti, Sr, Mn, Fe, P. The different samples from the three distinct
389 zones are grouped according to their provenance. They form three distinct clusters with no overlap
390 between their 80% significance level ellipses (fill) and minor overlaps between their 95% significance
391 ellipses (dash). It confirms the possibility to distinguish the provenance of the samples from their
392 geochemical signature.

393 Discrimination performed by LDA (Fig 3.B), for which the first axis accounts for 54.2 % and the second
394 for 45.8 %, is mostly driven by As, Cr (axis 1), K and Mn (axis 2) (ESI 8). Samples from the three
395 distinct zones are grouped according to their provenance forming three distinct groups with no overlap
396 between their 95% significance ellipses, making it a good model for sourcing ferruginous colouring
397 matters. LDA cross-validation provided a score of 87.3 % of correct attribution, confirming the
398 effectiveness of the model to discriminate the distinct zones.



408 Biplots of the first two components are presented in Fig 3.C and component loadings are given in ESI
409 7. For PCA (Fig. 3.C), the first two components account for 38 % of the total variation, mostly driven
410 by Cr, As, Zr, Sr, Al, Mn, Zn, Ga. Though samples from the three distinct zones are grouped according
411 to their provenance forming three identifiable poles, there are minor overlaps between the 80 %
412 significance level ellipses and rather large overlaps between the 95% ellipses.

413 Discrimination performed by LDA (Fig. 3.D), for which the first axes accounts for 74 % and the second
414 for 26 %, is mostly driven by Zn for both axes (ESI 9). Samples from the three distinct zones are grouped
415 according to their provenance forming three distinct groups with no overlap between their 95%
416 significance ellipses, making it a good model for sourcing ferruginous colouring matters. LDA cross-
417 validation for the PIXE datasets provided a score of 84.8% of correct attribution. Though smaller than
418 the ones obtained for ICP, the two cross-validation scores remain of same magnitude.

419 **3.d. pXRF results**

420 In total, 52 samples were analysed by pXRF (Table 1). Raw elemental concentration data are provided
421 in ESI 1. We first aimed to confirm the possibility to differentiate the three zones thanks to pXRF data.
422 Therefore, pXRF centred-log-ratio transformed data were submitted to principal component analysis
423 (PCA) and linear discriminant analysis (LDA) with the same elements as for the two precedent
424 analytical techniques.

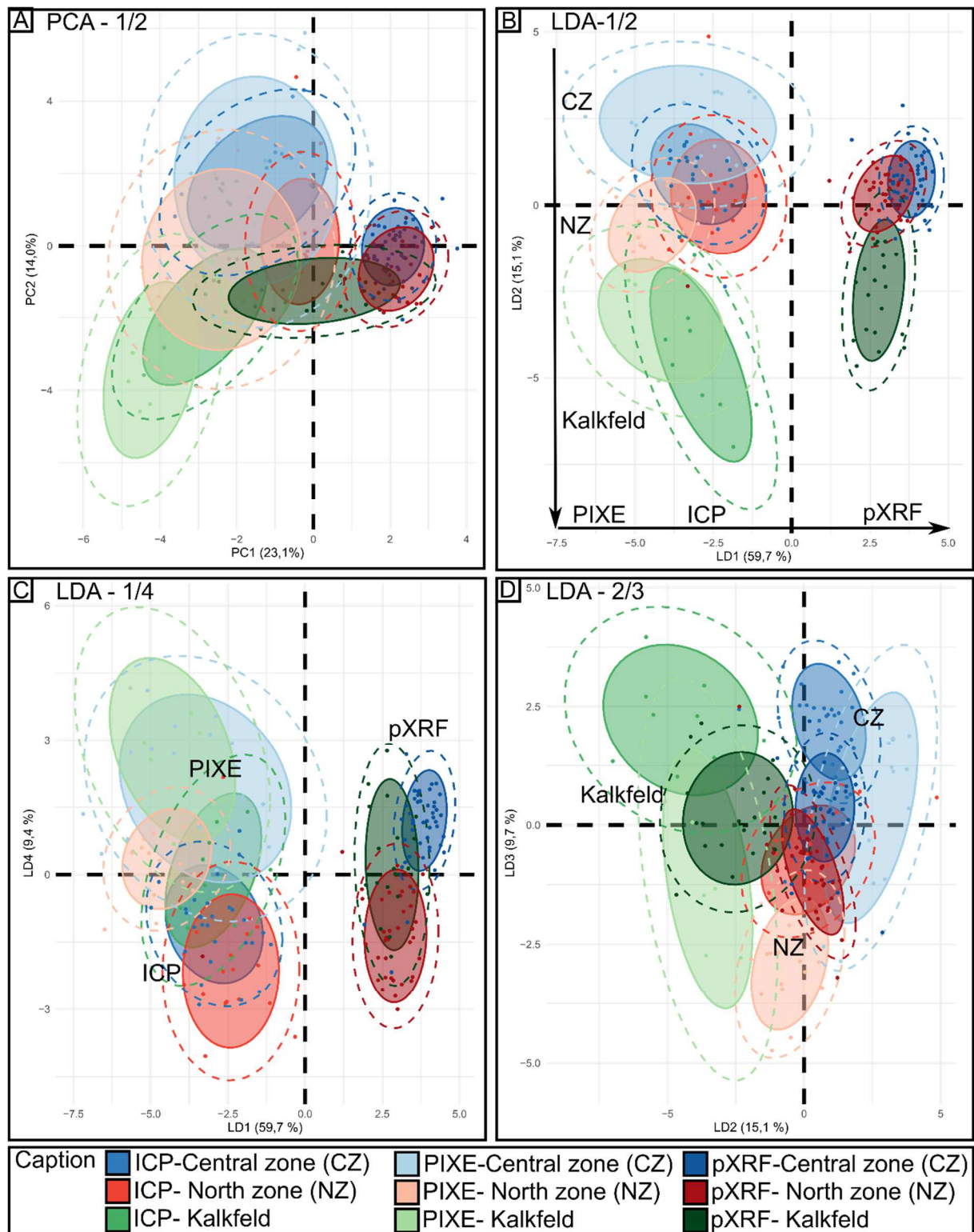
425 Biplots of the first two components are presented in Fig 3. E and component loadings are given in ESI
426 10. The two first PCA components account for 41 % of the total variation of the data, mostly driven by
427 Fe, Cu, Pb, K, Sr. Though the Kalkfeld samples stand out from CZ and NZ on the PCA biplots, there
428 are major overlaps between the 80 % significance level ellipses. The PCA performed on the “pXRF
429 centred-log-ratio” data (pXRF clr) fails to differentiate the three zones studied here.

430 Discrimination performed by linear discriminant analysis (LDA) (Fig. 3. F), for which the first axes
431 accounts for 54.5% and the second for 45.5%, is mostly driven by Al, Zn, Cu for both axes (ESI 10).
432 Samples from the three distinct zones are grouped according to their provenance forming three distinct
433 groups with no overlap between their 80% significance level ellipses (fill) and minor overlaps between
434 their 95% significance ellipses (dash). LDA cross-validation for the pXRF datasets provided a score of
435 70% of correct attribution. Smaller than the two previous cross-validation scores, the cross-validation
436 score also confirmed the lesser efficiency of the LDA with the pXRF data to discriminate the distinct
437 zones.

438 **3.d. Comparison of the datasets: Inter-equipment *versus* inter-zone variability**

439 We thence investigated the possibility to compare these datasets, evaluate the inter-equipment and inter-
440 zone variability. We first used our centred-log-ratio transformed dataset (clr) and submitted it to

441 principal components and linear discriminant analyses. Linear discriminant analyses factor consisted in
 442 the analytical technique used to measure the samples and the area of provenance of the samples (Fig. 4).
 443 PCA and LDA biplots are presented in Fig. 4 and variable loadings in ESI 11 and 12.



444

445 Fig. 4. Principal component analysis (A) and linear discriminant analysis (B-D) of the post merged
 446 standardized datasets from ICP, PIXE and pXRF. 80% significance level ellipses (fill) and minor
 447 overlaps between their 95% significance ellipses (dash). (double column, colour)

448

449 Biplot of the first two components of the PCA accounts for 37.1 % of the total variation of the data
450 (Fig.4.A). While the first component (23.1 %) mainly explains inter-equipment variability thanks to Ca,
451 Cr, Fe, Mn and W, the second component (14.0 %) tends to explain some inter-zone variability thanks
452 to Ti, Sr, Cu, Ni (ESI 11). From this biplot, it is clear that within the post merged standardized dataset,
453 the inter-equipment variability is higher than the inter-zone variability.

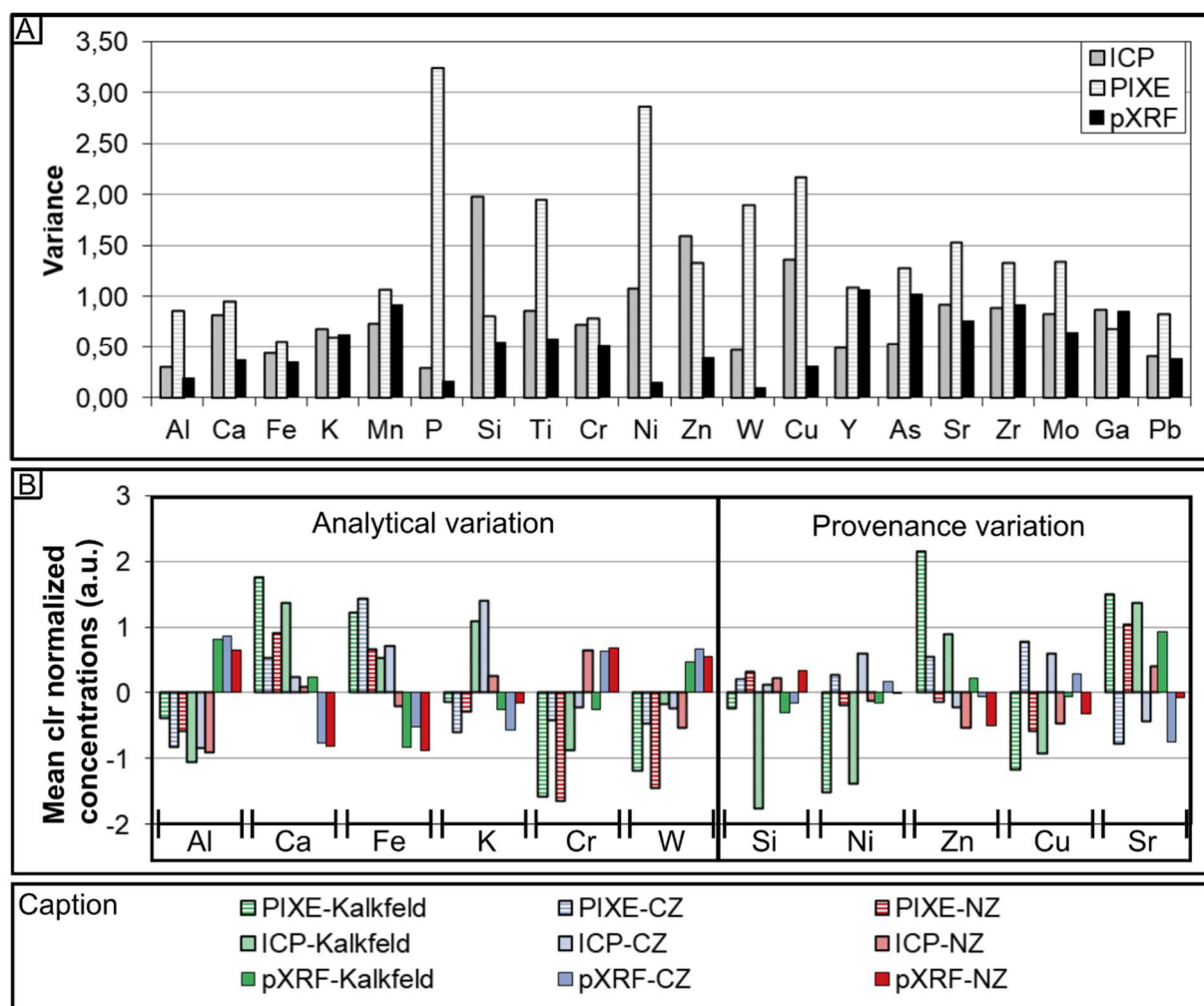
454 Biplots of the first four axes of the LDA help to go further into the analysis of the inter-equipment and
455 inter-zone variabilities (Fig 4.B-D). Two different trends appear on the LD1-LD2 biplot, one driven by
456 LD1 takes the inter-equipment variability, while the other one driven by LD2 takes the inter-zone
457 variability (Fig 4.B). On the LD1-LD4 biplot, two major poles tend to form according to the analysis
458 used to acquire the data pXRF on one side and PIXE and ICP on another (Fig. 4.C), while on the LD2-
459 LD3, the three poles correspond to the three zones of provenances of the samples (Fig. 4.D). While LD1
460 (59.7 %) and LD 4 (9.4 %) explains the inter-equipment variability, LD2 (15.1 %) and LD3 (9.7 %)
461 explains the inter-zone variability. The cross-validation performed thanks to the two first axes of the
462 LDA reached a score of 64.5%. In this case, 69.1 % of the dataset variation accounts for the inter-
463 equipment variability. In such conditions, centred-log-transformed normalisation is not suitable to
464 compare the data acquired by the different techniques.

465 As we wanted to understand which elements were driving the two different sources of variability of the
466 datasets, we analysed both the variance of the elements according to the analytical techniques used to
467 measure them and the mean values of each group defined as the combination of the zone of provenances
468 of the samples and the techniques used to analyse it. Results of these considerations are presented in
469 Fig. 5.

470 It appeared that the different analytical techniques presented different variances for each element.
471 Indeed, while iron and potassium displayed similar variance values around 0.5 for the three techniques,
472 the variances for P, Si, Ti, Ni, W and Cu present significant differences, ranging between 0.1 and 3.0
473 (Fig. 5.A).

474 Bar plot of the mean values of each of the nine groups defined (three zones and three analytical
475 techniques) permitted to confirm the two trends spotted on the LDA loadings, confirming Al, Ca, Fe, K,
476 Cr and W to be highly impacted by inter-equipment variability, while Si, Ni, Zn, Cu and Sr appeared to
477 discriminate more the zone of provenances of the samples (Fig. 5.B, ESI 12).

478 Though the inter-equipment variability of the post merged standardized dataset is too important to be
479 used to compare the samples analysed by the different analytical techniques, a part of the variance
480 appears to be driven by the geochemical properties of the provenance zones of the colouring matters.

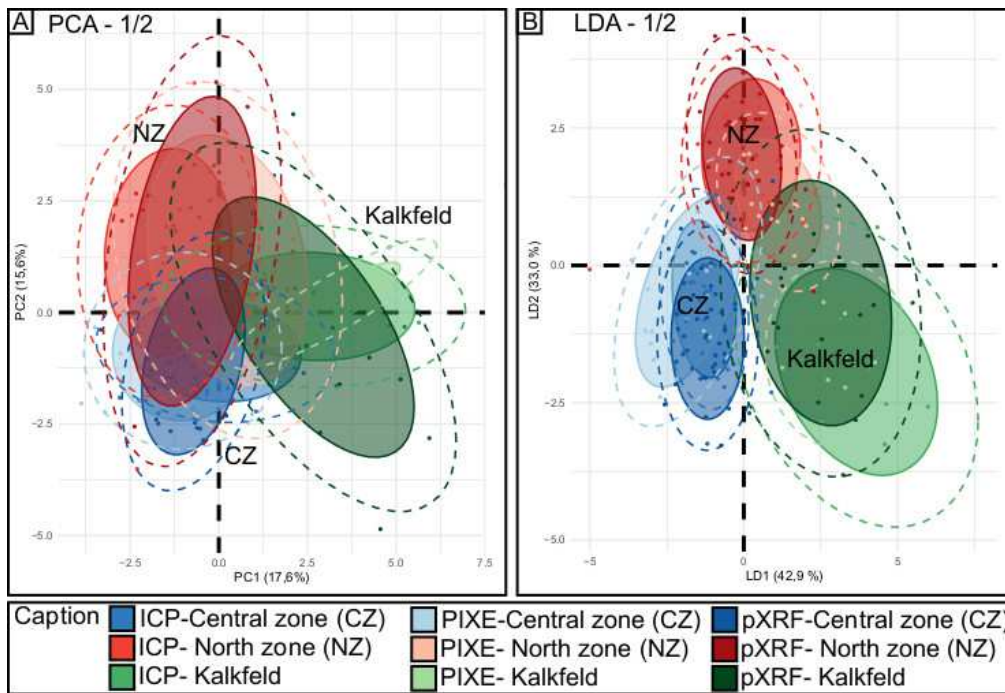


481

482 Fig. 5. A: Elemental concentration variance for each technique (ICP, PIXE and pXRF); B: Elemental
 483 variance for each technique and provenance zone on the post merged standardized dataset. (double
 484 column, colour)

485 3.e. Unification of the datasets

486 As demonstrated in the previous section, inter-equipment variability can be unneglectable and can
 487 induce a wide range of variance values for the same element. We standardize here each dataset separately
 488 before merging them. This procedure is a standardization that rescales the data sets to ensure the mean
 489 is 0 and the standard deviation 1. Corresponding PCA and LDA biplots are presented in Figure 6 and
 490 variable loadings in ESI 11 and 12.



491

492 Fig. 6. Principal component analysis (A) and linear discriminant analysis (B) of the pre merged
 493 standardized datasets established by ICP, PIXE and pXRF. 80% significance level ellipses (fill) and
 494 minor overlaps between their 95% significance ellipses (dash). (double column, colour)

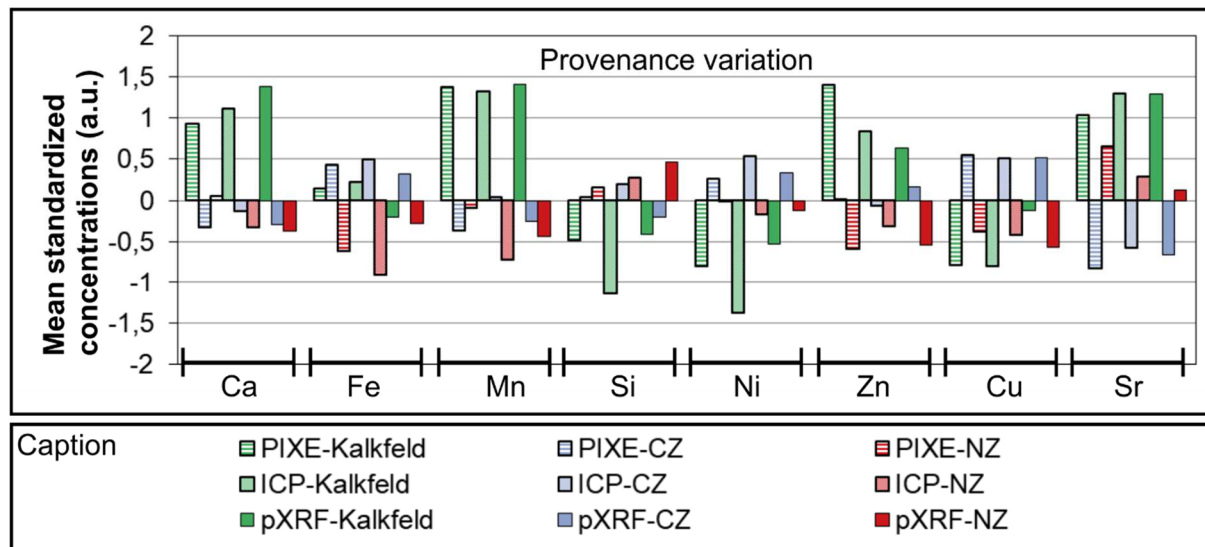
495

496 Biplot of the first two components of the PCA accounts for 33.2 % of the total variation of the data.
 497 Though there are major overlaps between the 80% significance level ellipses, three poles appear on the
 498 PC1-PC2 biplot. These three poles correspond to the zones of provenance of the samples. While the first
 499 component (17.6 %) mainly differentiates the Kalkfeld zone from the two others thanks to Cr, Ca, Mn,
 500 Sr, As, Zn, the second component (15.6 %) tends to differentiate the NZ and CZ zones thanks to Fe, Ti,
 501 Zr, Si, Cu (ESI 11). These biplots demonstrate that inter-equipment variability can be minimized by
 502 applying a standardization procedure of each dataset acquired with each technique before merging them.

503 As for the LDA, the LD1-LD2 axes account for 75.9 % of the total variation of the data. Although we
 504 tried to distinguish nine groups, and despite a slight overlap of the 80% significant level ellipses for
 505 Kalkfeld pXRF and NZ data, three poles can be distinguished according to the zone of provenances of
 506 the samples (Fig. 6). The cross-validation performed on the two first axes of the LDA reached a score
 507 of 75.2%, even reaching 82.5% when all axes are considered. Thus, the standardization considerably
 508 increased the discrimination of the zones, reaching the same cross-validation score magnitude than what
 509 had been obtained for ICP or PIXE alone. It allows a comparison of the data acquired with the different
 510 analytical techniques.

511 Bar plot of the variance values of each of the nine groups defined (three zones and three analytical
 512 techniques) permitted to confirm that the standardization procedure permitted to minimize the inter-

513 equipment variability (Fig. 7). After the standardization procedure, none of the elements highlighted an
 514 inter-equipment variability, while eight elements differentiated the groups according to the provenance
 515 zones of the samples. Elements such as Ca and Fe, which were highly impacted by the inter-equipment
 516 variability, even contributed to differentiate the zone of provenances of the samples.



517

518 Fig. 7. Elemental variance for each technique and provenance zone on the pre merged standardized
 519 dataset. (double column, colour)

520 4.DISCUSSION

521 Measures performed on standards (diorite DRN, bauxite BXN and iron formation IFG) confirmed ICP-
 522 MS is the most accurate and repeatable analytical technique (Table 3), followed by ICP-OES and PIXE.
 523 pXRF measured data present some discrepancies with the certified values, as already stated in the
 524 literature (Hein et al., 2002). Although the discrepancies observed for the two standards are weak, it
 525 appeared that data acquired with these techniques were not directly comparable. This is not surprising
 526 as inter-laboratories and sometimes day to day measure on a same equipment are not directly combinable
 527 (Yellin et al., 1978 ; Popelka-Filcoff et al., 2012 ; Salomon et al., 2016)..

528 Published comparisons of data acquired by sundry techniques usually compare the performances of each
 529 analytical techniques to differentiate for example ceramic workshops (Hein et al., 2002 ; Grave et al.,
 530 2005 ; Speakman et al., 2011 ; Mitchell et al., 2012) or mineral outcrops (Kasztovszky et al., 2018).
 531 They all tend to prove the consistency between the cluster performed thanks to NAA, ICP-OES/ICP-
 532 MS, PIXE and pXRF analytical methods. Here we demonstrate this consistency to be also true for
 533 Namibian ferruginous colouring matters. We go further by comparing the datasets, allowing us to
 534 determine the importance of the elemental inter-equipment and inter-zones variabilities.

535 Application of the centred-log-ratio transformed data and multivariate statistics revealed that ICP-
 536 OES/ICP-MS and PIXE analyses could differentiate the Namibian samples according to their zone of

537 origin (Fig. 2). Using pXRF measurements, three distinct poles corresponding to the three zones of
538 origin of the samples considered in our study can be observed, slightly overlapping each other. Though
539 quick to acquire, pXRF analyses require time and efforts to quantify the elemental composition of
540 ferruginous colouring matters (Speakman et al., 2013). Having the possibility to compare them with
541 other techniques compensates in some views the time and efforts invested to process them.

542 In a recent paper, Chanteraud and colleagues (2021) investigated the capacities of pXRF to study the
543 “*chaîne opératoire*” of ferruginous colouring matters. They compared pXRF data to PIXE and ICP data
544 as well and conclude that it is currently not possible to directly use pXRF data to accurately quantify the
545 elemental content of colouring matters or to discriminate different raw materials. Our study confirms
546 the difficulty to compare the concentration calculated with pXRF with the results obtained with PIXE
547 or ICP-MS. The comparison of raw closed and merged data show that the analytical inter-equipment
548 variability accounts for most of the total variability of the data (Fig. 3). Compositional differences
549 related to geological discriminations can exist. They are partially masked by the preponderant inter-
550 equipment variability. This inter-equipment variability is mainly due to the difference of measurement
551 principles between the distinct techniques used, leading to analyse different volumes, to make some
552 elements difficult to measure.

553 This does not mean that some of our data are invalid as explained by Bernard (2017). Scales between
554 the measures might be different and therefore need to be corrected, so they can be considered valid and
555 compatible with other data. As we noticed differences between the determined variances of the elements
556 according to the analytical techniques (Fig. 5), we standardized our data according to the analytical
557 technique used so that all elements present a variance equal to one. This standardization was performed
558 separately for each dataset collected through distinct analytical techniques. Doing so minimized the
559 inter-equipment variability and allowed a comparison between the data acquired by pXRF, PIXE and
560 ICP-OES/ICP-MS (Fig. 6). Two facts must be noticed: 1) we did not reduce our number of variables,
561 consequently favouring better discrimination of the groups, not only according to the provenance of the
562 samples but also the techniques used to perform the measures; 2) we used centred log-ratio transformed
563 data so that the study is robust to the fact we analysed sub-compositions of our samples (Aitchison, 1982
564 ; Baxter et al., 2005). As our study is robust to sub-composition statistical analyses, a similar conclusion
565 could be obtained with the Fe log-ratio transformation usually used in ferruginous colouring matter
566 sourcing studies (David et al., 1993 ; Popelka-Filcoff et al., 2007, 2008).

567 Such a geochemical discrimination study is largely favoured by the geological context of Central
568 Namibia, characterized by different tectonostratigraphic regions. Here, we analysed materials coming
569 from three of the central Namibian tectonostratigraphic regions: Central Zone where lies numerous rock
570 art sites such as Leopard Cave, Kalkfeld complex located 100 km north to Leopard Cave, and North
571 Zone located at more than 100 km north-west from Leopard Cave (Figure 1). Our previous study has

572 proved, some of the collected but unmodified colouring matters recovered at Leopard Cave come from
573 the Central Zone and the North Zones (Mauran et al., 2021a) . Thanks to the present standardization
574 procedure, integration of other tectonostratigraphic zones could be implemented in the future. Using the
575 standardization procedure on Leopard Cave materials, rich of numerous massive haematite (Mauran et
576 al., 2020) , would allow us to understand better if past populations who occupied the site preferred to
577 use specific massive haematite and if different haematite were used for different purposes, thus
578 providing a better understanding of past populations behaviours. It would be interesting to investigate
579 the possibility to perform such a comparison at a lower geographical level within the different
580 tectonostratigraphic zones to differentiate the sundry outcrops. The present unification is already of great
581 help since it allows us to investigate the possible existence of large procurement networks of raw
582 colouring matters in Namibia. Investigating if such unification could be performed in a different
583 geological context would be of higher interest, it could help us to ensure the standardization procedure
584 is robust.

585 It is worth mentioning that our standardization procedure should be only deployed in other contexts and
586 on other materials after ensuring that standards and references analysed through the different analytical
587 techniques considered are comparable. The standardization procedure is then a way to include modified
588 and unmodified ferruginous colouring matters in provenance studies, which allows a better
589 understanding of past populations behaviours towards the exploitation of these raw materials.

590 This comparison of the datasets acquired by distinct analytical techniques opens the possibility to
591 establish a geochemical provenance model of Namibian ferruginous colouring matters from different
592 analytical techniques. Large assemblages of archaeological materials are usually screened by the non-
593 invasive and easily accessible pXRF technique. Our standardization procedure allows the integration of
594 these pXRF data to provenance study and validates the coherence of performing such pre-screening
595 analyses for ferruginous colouring matters as sometimes performed for iron slags (Vega et al., 2019) .
596 pXRF data were acquired with an equipment calibrated thanks to 21 standards, most of which did not
597 match the composition of the geological samples. With the use of standards matching better the
598 composition of the considered samples, the pXRF accuracy should be improved,

599 Using the pXRF technique on both geological and archaeological collections would provide some first
600 data to better understand the samples. In specific context such the one studied by Lebon and colleagues
601 (2019), pXRF can reveal specific geochemical patterns. These patterns could be further investigated and
602 confirmed on a smaller batch of samples, wisely selected from petrographic observations and pXRF
603 analyses, through invasive techniques such as ICP-OES/ICP-MS or NAA. Thence, it is possible to
604 compare these precise geochemical signatures with data acquired on archaeological samples, chosen
605 thanks to reasoned sampling strategy using pXRF pre-screening results, with both non-invasive
606 analytical techniques such as PIXE for the samples presenting anthropic modifications and invasive

607 techniques for some unmodified archaeological pieces. Thus, the pXRF could help researchers to
608 perform their sampling procedure for the time or fund costly analyses such as ICP-OES/ICP-MS or
609 NAA. Naturally, these techniques should then be combined with other analytical methods such as
610 petrography or X-ray diffractometry. Such multimodal approaches are the way to go to understand as
611 much as possible the “*chaîne opératoire*” of ferruginous colouring materials exploitation (Dayet, 2021
612 ; Domingo and Chieri, 2021).

613 Furthermore, our standardization procedure could offer a way to compare data derived from different
614 non-invasive and invasive analytical techniques on the same colouring matter fragments. Doing so, it
615 would permit to take the best of each technique. Indeed, it would then be possible to take advantage of
616 the accessibility, rapidity, portability and non-invasiveness of the pXRF, or of the accuracy, spatial
617 resolution and non-invasiveness of the PIXE together with the accessibility, micro-destructive, high-
618 precision and rapidity of the ICP-OES and ICP-MS. Thanks to this data unification, it would thence
619 possible to have a better understanding of large ferruginous colouring matter assemblages, the first step
620 toward a better understanding of the “*chaîne opératoire*” link to these materials. It would thence here
621 possible to have an accurate knowledge of the chemical fingerprint of the potential sources and compare
622 it to some non-destructive PIXE analyses carried out on archaeological pieces.

623 Future studies should focus on ferruginous residue analyses thanks to PIXE and LA-ICP-MS/MS (or
624 NAA) and the way to compare them with ferruginous colouring samples to offer a way to study the
625 whole “*chaîne opératoire*” linked to ferruginous colouring matter as presented in Fig. 1. These
626 developments should be carried out together with petrological and SEM observations to offer robust
627 ways to study ferruginous colouring matters (Dayet et al., 2013 ; Salomon et al., 2016) . Used together
628 with these developments, our standardization procedure offers a way to set up a robust “grain per grain”
629 microscopic methodology. This methodology could tackle the intrinsic heterogeneity of ferruginous
630 colouring matter, through the multiplication of the analyses on the same sample as mentioned for LA-
631 ICP-MS by Scadding and colleagues (2015).

632 Finally, such a standardization allows comparison of compositional datasets acquired by distinct users,
633 increasing the interoperability of the datasets, a key idea of the FAIR concept (Findable, Accessible,
634 Interoperable, Reusable) for better practices in science. With our standardization procedure, it is possible
635 to minimize the inter-equipment variability, including the inter-operators one, and compare datasets
636 from different origins. Therefore, our standardization offers a new way to increase the interoperability
637 and reusability of the datasets acquired at different laboratories or by different teams, which has been a
638 preoccupation for archaeometry laboratory in the last two decades (Glascock et al., 2004). Naturally, to
639 do so it is of utmost importance to use the same standards between the datasets to be compared, as
640 already mentioned by Salomon and colleagues (2016). Comparison of the standards will confirm that
641 on similar samples the data acquired on distinct equipment are coherent and comparable.

642 **5.CONCLUSIONS**

643 In this article, we first investigated the issue of data standardization to compare elemental analyses
644 acquired by distinct analytical techniques. Second, we tested the efficiency of each technique to
645 discriminate the source of ferruginous colouring matter sampled in three different geological zones when
646 coupled to multivariate statistical analyses. Third, we evidenced how the datasets can be incompatible
647 though they are precise and accurate. Fourth, we demonstrated the possibility to merge the multivariate
648 analyses through a basic data transformation. Five, we discussed the archaeological implication and
649 limitation of our methodology.

650 The results of the study indicated that using the presented standardization of the measured elemental
651 concentrations could be used to obtain a unified dataset in which inter-equipment variability is
652 negligible. In doing so, it allowed the use of multivariate analyses to differentiate Namibian ferruginous
653 colouring matter provenance.

654 Moreover, it opens the way for building a multi-analytical provenance model. Such a multi-analytical
655 provenance model would gather more analyses than the ones usually performed and relying on a unique
656 invasive technique (Kiehn et al., 2007 ; Popelka-Filcoff et al., 2007, 2008 ; Dayet et al., 2013 ; Eiselt et
657 al., 2011 ; MacDonald et al., 2013, 2018 ; Pierce et al., 2020 ; Dayet, 2021). Overcoming this number
658 limitation is crucial to perform more robust provenance studies for ferruginous colouring matter on the
659 model of what has been done for iron slags in metallurgy (Leroy, 2010 ; Leroy et al., 2012). Such studies
660 do not only rely on a sole generic multivariate analysis but go beyond evaluating for each sample the
661 statistical possibility that a sample can come from a specific mining region. Doing so, better take into
662 account the possibility that some outcrops used by past populations are nowadays depleted. As the
663 statistical tests used to do so (mainly linear discriminant analysis) require the comparison of distinct
664 distributions (ideally normal distributions), each archaeological sample should be represented by a
665 distribution of analyses. The cost and time required to do this with a unique invasive technique are
666 tremendous and explain why it has so far never been performed. Through this unification procedure,
667 each archaeological sample could easily be represented by a distribution. As we are convinced, studies
668 on ferruginous colouring matters should go towards this direction, our future research will focus on the
669 possibility to use our multi-technical tectonostratigraphic zone discrimination model to perform such
670 provenance analyses. However, comparing and unifying the data is different than performing
671 provenance analyses and further work are necessary to ensure such an approach would fulfil the
672 Provenance Postulate (Weigand, 1977).

673 Beyond the possibility to perform robust provenance studies, this unification of the datasets allows
674 provenance studies to be anchored into the investigation of ferruginous colouring matters evolutive
675 chain as defined for siliceous resources by Fernandes and colleagues (2008) . Such an approach is crucial

676 when studying the social-cultural behaviours of past populations. As stated by Fernandes and colleagues
677 (2008), identifying characteristic specific to secondary beds, called “gitological types” is more useful
678 than “genetic types” which depend upon the initial geological formations from which the ferruginous
679 colouring matter come from for provenance studies. To this aspect, our results are crucial for general
680 geochemical analyses studies of archaeological materials and cultural material analyses. Our result will
681 enable inter-study comparisons of new analytical techniques or procedures applied to sourcing research
682 and existing techniques applied to new materials or geographic regions.

683 **CONFLICT OF INTEREST STATEMENT**

684 There are no conflicts to declare.

685 **AUTHOR CONTRIBUTIONS**

686 Conceptualization: GM, ML, LB, FD, BC, DP, JJB, CN

687 Data curation: GM, BC, ML

688 Formal analysis: GM, BC, LB, ML

689 Funding acquisition: ML, DP, JJB, BC, LB

690 Investigation: GM

691 Methodology: GM, ML, LB, FD, BC, JJB, CN

692 Project administration: GM, ML, BC, DP, JJB

693 Resources: GM, OT, ML, BC, FD, DP, LB, CN

694 Supervision: ML, JJB

695 Validation: BC, ML, FD, JJB, LB, OT

696 Visualization: GM

697 Writing – original draft: GM

698 Writing – review & editing: GM, ML, JJB, FD, DP, BC, LB, OT

699 **ACKNOWLEDGEMENTS**

700 The authors are very grateful to Ms and Mr Rust and their family for their kind permission to access and excavate
701 the archaeological site of Leopard Cave, located on their farm.

702 This research was supported by grants from the French Ministry of Foreign Affairs through the project “MANAM:
703 Mission Archéologique en NAMibie”, the LaBex BCDiv (Biological and Cultural Diversity) for the project
704 “Dynamique des peuplement en Namibie à l'Holocène - NAMIBIE (Windhoek, Erongo)” both directed by D.P.,
705 the Observatoire des Patrimoines de Sorbonnes universités (OPUS) through the project “APaNam: Art rupestre et
706 Patrimoine en Namibie” directed by M.L. Research by G.M. was funded by the Chaire Polyre of Sorbonnes
707 Universités.. Permission to conduct research was granted by the National Heritage Council of Namibia (permit
708 11/2015 and permit renewal 04/2017 given to D.P.) and the Namibian Ministry of Mine and Energy (permit ES
709 31957 granted to G.M.). We are grateful for the support and assistance of this institution as well as the National
710 Museum of Namibia, the National Heritage Council, the Geological Survey of Namibia and the French embassy
711 in Namibia. We are grateful to Quentin Pichon and Clare Pachecaud for the help with the air-extracted PIXE
712 analyses at the NEWAGLAE facility. We also acknowledge the two anonymous reviewers who helped us improve
713 the manuscript.

714 GM acknowledges the support of the DSI-NRF Center of Excellence in Paleosciences (CoE-Pal) towards his
715 postdoctoral work when this paper was written and corrected. Opinions expressed and conclusions arrived at, are
716 those of the author and are not necessarily to be attributed to the CoE. Opinions expressed and conclusions arrived
717 at, are those of the authors and are not necessarily to be attributed to the CoE.

718 **REFERENCES**

719 Aitchison, J., 1982. The statistical analysis of compositional data. *Journal of the Royal Statistical Society: Series*
720 *B (Methodological)*, 44(2):139–160. <https://doi.org/10.1111/j.2517-6161.1982.tb01195.x>.

721 Aitchison, J., 1986. *The Statistical Analysis of Compositional Data. Monographs on Statistics and Applied*
722 *Probability*. London, Chapman, & Hall Ltd.

723 Baxter, M. J., 1994. *Exploratory multivariate analysis in archaeology*. Edinburgh University Press.

724 Baxter, M. J., 1995. Standardization and transformation in principal component analysis, with applications to
725 archaeometry. *Journal of the Royal Statistical Society: Series C (Applied Statistics)*, 44(4), 513-
726 527. <https://doi.org/10.2307/2986142>.

727 Baxter, M. J., Cool, H. E. M., Jackson, C. M., 2005. Further studies in the compositional variability of colourless
728 Romano-British vessel glass. *Archaeometry*, 47(1), 47-68. <https://doi.org/10.1111/j.1475-4754.2005.00187.x>.

729 Beck, L., Lebon, M., Pichon, L., Menu, M., Chiotti, L., Nespoulet, R., Paillet, P., 2011. PIXE characterisation of
730 prehistoric pigments from Abri Pataud (Dordogne, France). *X-Ray Spectrometry*, 40(3), 219-223.
731 <https://doi.org/10.1002/xrs.1321>.

732 Beck, L., Salomon, H., Lahlil, S., Lebon, M., Odin, G. P., Coquinot, Y., Pichon, L., 2012. Non-destructive
733 provenance differentiation of prehistoric pigments by external PIXE. *Nuclear Instruments and Methods in*

- 734 Physics Research Section B: Beam Interactions with Materials and Atoms, 273, 173-177.
735 <https://doi.org/10.1016/j.nimb.2011.07.068>.
- 736 Bernard, H. R., 2017. Research methods in anthropology: Qualitative and quantitative approaches. Rowman &
737 Littlefield.
- 738 Bernatchez, J. A., 2008. Geochemical characterization of archaeological ochre at Nelson Bay Cave (Western
739 Cape Province), South Africa. *South African Archaeological Bulletin*, 63(187), 3-11.
740 <https://search.informit.org/doi/10.3316/informit.485994972962238>.
- 741 Blanca, M. J., Arnau, J., López-Montiel, D., Bono, R., Bendayan, R., 2013. Skewness and kurtosis in real data
742 samples. *Methodology*. <https://doi.org/10.1027/1614-2241/a000057>
- 743 Buxeda i Garrigós, J., 2018. Compositional Data Analysis, in Varela et al. (Eds.), *The Encyclopedia of*
744 *Archaeological Sciences*, Wiley Blackwell, Chichester, pp.1-5.
- 745 Cain, M. K., Zhang, Z., Yuan, K. H., 2017. Univariate and multivariate skewness and kurtosis for measuring
746 nonnormality: Prevalence, influence and estimation. *Behavior research methods*, 49(5), 1716-1735.
747 <https://doi.org/10.3758/s13428-016-0814-1>
- 748 Chalmin, E., Huntley, J., 2018. Characterizing rock art pigments. In : Bruno David; Ian J. McNiven (Eds). *The*
749 *Oxford Handbook of the Archaeology and Anthropology of Rock Art*, Oxford Handbook,
750 [http://www.oxfordhandbooks.com/view/10.1093/oxfordhb/9780190607357.001.0001/oxfordhb-9780190607357-](http://www.oxfordhandbooks.com/view/10.1093/oxfordhb/9780190607357.001.0001/oxfordhb-9780190607357-e-48)
751 [e-48](http://www.oxfordhandbooks.com/view/10.1093/oxfordhb/9780190607357.001.0001/oxfordhb-9780190607357-e-48), 2018,
- 752 Chalmin, E., Scmitt, B., Chanteraud, C., Chassin de Kergommeaux, A., Soufi, F., Salomon, H., 2021, How to
753 distinguish red coloring matter used in prehistoric time? The contribution of visible near-infrared diffuse
754 reflectance spectroscopy, *Color Res. Appl.*, 46(3), 653-673. <https://doi.org/10.1002/col.22647>.
- 755 Chanteraud, C., Chalmin, E., Lebon, M., Salomon, H., Jacq, K., Noûs, C., Delannoy, J.J., Monney, J., 2021.
756 Contribution and limits of portable X-ray fluorescence for studying Palaeolithic rock art: a case study at the
757 Points cave (Aigueze, Gard, France). *J. Archaeol. Sci. Rep.*, 37, 102898.
758 <https://doi.org/10.1016/j.jasrep.2021.102898>.
- 759 Chessel, D., Dufour, A. B., Thioulouse, J., 2004. The ade4 package-I-One-table methods. *R news*, 4(1), 5-10.
- 760 David, B., Clayton, E., Watchman, A., 1993. Initial results of PIXE analysis on northern Australian
761 ochres. *Australian Archaeology*, 36(1), 50-57
- 762 Dayet, L., 2012. Matériaux, transformations et fonctions de l'ocre au Middle Stone Age: le cas de Diepkloof
763 Rock Shelter dans le contexte de l'Afrique australe, PhD Dissertation, Université de Bordeaux I, Bordeaux.
764 <https://tel.archives-ouvertes.fr/tel-00814875/>.
- 765 Dayet, L., 2021. Invasive and Non-Invasive Analyses of Ochre and Iron-Based Pigment Raw Materials: A
766 Methodological Perspective, *Minerals*, 11(2), 210. <https://doi.org/10.3390/min11020210>.
- 767 Dayet, L., Texier, P. J., Daniel, F., Porraz, G., 2013. Ochre resources from the middle stone age sequence of
768 Diepkloof Rock Shelter, Western Cape, South Africa. *Journal of Archaeological Science*, 40(9), 3492-
769 3505. <https://doi.org/10.1016/j.jas.2013.01.025>.
- 770 Dayet, L., Le Bourdonnec, F. X., Daniel, F., Porraz, G., Texier, P. J., 2016. Ochre provenance and procurement
771 strategies during the middle stone age at Diepkloof Rock Shelter, South Africa. *Archaeometry*, 58(5), 807-
772 829. <https://doi.org/10.1111/arcm.12202>.
- 773 Domingo, I., & Chieli, A., 2021. Characterizing the pigments and paints of prehistoric artists. *Archaeological*
774 *and Anthropological Sciences*, 13(11), 1-20. <https://doi.org/10.1007/s12520-021-01397-y>

- 775 Eiselt B, Popelka-Filcoff RS, Darling A, Glascock M., 2011. Hematite sources and archaeological ochres from
776 Hohokam and O’odham sites in Central Arizona: an experiment in type identification and characterization. *J*
777 *Archaeol Sci* 38:3019–3028
- 778 Eiselt, B. S., Dudgeon, J., Darling, J. A., Paucar, E. N., Glascock, M. D., Woodson, M. K., 2019. In-situ sourcing
779 of hematite paints on the surface of hohokam red-on-Buff ceramics using laser ablation–inductively coupled
780 plasma–mass spectrometry (LA–ICP–MS) and instrumental neutron activation analysis. *Archaeometry*, 61(2),
781 423-441. <https://doi.org/10.1111/arcm.12427>.
- 782 Enserro, D. M., Demler, O. V., Pencina, M. J., D’Agostino Sr, R. B., 2019. Measures for evaluation of
783 prognostic improvement under multivariate normality for nested and nonnested models. *Statistics in medicine*,
784 38(20), 3817-3831. <https://doi.org/10.1002/sim.8204>
- 785 d’Errico, F., 2003. The Invisible Frontier: A Multiple Species Model for the Origin of Behavioral Modernity,
786 *Evol. Anthropol.* 12, 188–202. <https://doi.org/10.1002/evan.10113>.
- 787 Fernandes, P., Raynal, J.-P., Moncel, M.-H., 2008. Middle palaeolithic raw material gathering territories and
788 human mobility in the southern massif central, france : first result from a petro-archaeological study on flint.
789 *Journal of Archaeological Science*, 35(8), 2357–2370. <https://doi.org/10.1016/j.jas.2008.02.012>.
- 790 Glascock, M. D., Neff, H., Vaughn, K. J., 2004. Instrumental neutron activation analysis and multivariate
791 statistics for pottery provenance. *Hyperfine Interactions*, 154(1), 95-105.
792 <https://doi.org/10.1023/B:HYPE.0000032025.37390.41>.
- 793 Grave, P., Lisle, L., Maccheroni, M., 2005. Multivariate comparison of ICP-OES and PIXE/PIGE analysis of
794 east Asian storage jars. *Journal of Archaeological Science*, 32(6), 885-896.
795 <https://doi.org/10.1016/j.jas.2005.01.011>.
- 796 Green, R. L., Watling, R. J., 2007. Trace element fingerprinting of Australian ochre using laser ablation
797 inductively coupled plasma-mass spectrometry (LA-ICP-MS) for the provenance establishment and
798 authentication of indigenous art. *Journal of forensic sciences*, 52(4), 851-859. <https://doi.org/10.1111/j.1556-4029.2007.00488.x>.
- 800 Heginbotham, A., Bassett, J., Bourgarit, D., Eveleigh, C., Glinsman, L., Hook, D., Smith, D., Speakman, R. J.,
801 Shugar, A., Van Langh, R., 2015. The C opper CHARM S et: A New S et of Certified Reference Materials for
802 the Standardization of Quantitative X-Ray Fluorescence Analysis of Heritage C opper Alloys. *Archaeometry*,
803 57(5), 856-868. <https://doi.org/10.1111/arcm.12117>
- 804 Hein, A., Tsolakidou, A., Iliopoulos, I., Mommsen, H., i Garrigós, J. B., Montana, G., Kilikoglou, V., 2002.
805 Standardisation of elemental analytical techniques applied to provenance studies of archaeological ceramics: an
806 inter laboratory calibration study. *Analyst*, 127(4), 542-553. <https://doi.org/10.1039/B109603F>.
- 807 Hodgskiss, T., 2010. Identifying Grinding, Scoring and Rubbing Use-Wear on Experimental Ochre Pieces. *J.*
808 *Archaeol. Sci.* 37(12), 3344–3358. <https://doi.org/10.1016/j.jas.2010.08.003>.
- 809 Hodgskiss, T., 2014. The Cognitive Requirements for Ochre Use in the Middle Stone Age at Sibudu, South
810 Africa. *Camb. Archaeol. J.* 24(3), 405–428. <https://doi.org/10.1017/S0959774314000663>.
- 811 Huntley, J., 2021. Australian Indigenous ochres: Use, sourcing, and exchange. *The Oxford Handbook of the*
812 *Archaeology of Indigenous Australia and New Guinea*. Oxford: Oxford University Press. <https://doi.org/10.1093/oxfordhb/9780190095611.013>, 21.
- 814 Iriarte, E., Foyo, A., Sánchez, M. A., Tomillo, C., Setién, J., 2009. The origin and geochemical characterization
815 of red ochres from the Tito Bustillo and Monte Castillo caves (northern Spain). *Archaeometry*, 51(2), 231-
816 251. <https://doi.org/10.1111/j.1475-4754.2008.00397.x>.

- 817 Jercher, M., Pring, A., Jones, P. G., Raven, M. D., 1998. Rietveld X-ray diffraction and X-ray fluorescence
818 analysis of Australian aboriginal ochres. *Archaeometry*, 40(2), 383-401. [https://doi.org/10.1111/j.1475-](https://doi.org/10.1111/j.1475-4754.1998.tb00845.x)
819 4754.1998.tb00845.x.
- 820 Kasztovszky, Z., Maróti, B., Harsányi, I., Párkányi, D., Szilágyi, V., 2018. A comparative study of PGAA and
821 portable XRF used for non-destructive provenancing archaeological obsidian. *Quaternary International*, 468,
822 179-189. <https://doi.org/10.1016/j.quaint.2017.08.004>.
- 823 Kiehn, A. V., Brook, G. A., Glascock, M. D., Dake, J. Z., Robbins, L. H., Campbell, A. C., Murphy, M. L. 2007.
824 Fingerprinting specular hematite from mines in Botswana, Southern Africa, in: M.D Glascock, R.J. Speakman,
825 R.S. Popelka-Filcoff (Eds.), *Archaeological Chemistry: Analytical Techniques and Archaeological*
826 *Interpretation*, ACS Symposium Series 968, American Chemical Society, Washington DC, 2007, pp. 460-479.
- 827 Korkmaz, S., Goksuluk, D., Zararsiz, G., 2014. MVN: An R package for assessing multivariate normality. *The R*
828 *Journal*, 6(2), 151-162.
- 829 Lebon, M., Beck, L., Grégoire, S., Chiotti, L., Nespoulet, R., Menu, M., Paillet, P., 2014. Prehistoric pigment
830 characterisation of the Abri Pataud rock-shelter (Dordogne, France). *Open journal of Archaeometry*, 2(1).
831 <https://doi.org/10.4081/arc.2014.5456>.
- 832 Lebon, M., Pichon, L., Beck, L., 2018. Enhanced identification of trace element fingerprint of prehistoric
833 pigments by PIXE mapping. *Nuclear Instruments and Methods in Physics Research Section B: Beam*
834 *Interactions with Materials and Atoms*, 417, 91–95. <https://doi.org/10.1016/j.nimb.2017.10.010>
- 835 Lebon, M., Gallet, N., Bondetti, M., Pont, S., Mauraun, G., Walter, P., Bellot-Gurlet, L., Puaud, S., Zazzo, A.,
836 Forestier, H., Auetrakulvit, P., Zeitoun, V., 2019. Characterization of painting pigments and ochers associated to
837 Hoabinhian archaeological context at the rock paintings site of Doi Pha Kan (Thailand). *J. Archaeol. Sci. Rep.*,
838 26, 101855. <https://doi.org/10.1016/j.jasrep.2019.05.020>.
- 839 Leroy, S., 2010. *Circulation au moyen âge des matériaux ferreux issus des Pyrénées ariégoises et de la*
840 *Lombardie. Apport du couplage des analyses en éléments traces et multivariés*. Doctoral Dissertation, Université
841 de Technologie de Belfort-Montbéliard. <https://tel.archives-ouvertes.fr/tel-00598796>.
- 842 Leroy, S., Cohen, S., Verna, C., Gratuze, B., Téreygeol, F., Fluzin, P., Bertrand, L., Dillmann, P., 2012. The
843 medieval iron market in Ariège (France). Multidisciplinary analytical approach and multivariate analyses. *J.*
844 *Archaeolog. Sci.*, 39(4), 1080–1093. <https://doi.org/10.1016/j.jas.2011.11.025>.
- 845 MacDonald, B. L., Hancock, R. G. V., Cannon, A., Pidruczny, A., 2011. Geochemical characterization of ochre
846 from central coastal British Columbia, Canada. *Journal of Archaeological Science*, 38(12), 3620-3630.
- 847 MacDonald, B. L., Hancock, R. G. V., Cannon, A., McNeill, F., Reimer, R., Pidruczny, A., 2013. Elemental
848 analysis of ochre outcrops in southern British Columbia, Canada. *Archaeometry*, 55(6), 1020-1033.
849 <https://doi.org/10.1111/j.1475-4754.2012.00719.x>.
- 850 MacDonald, B. L., Fox, W., Dubreuil, L., Beddard, J., Pidruczny, A., 2018. Iron oxide geochemistry in the Great
851 Lakes Region (North America): Implications for ochre provenance studies. *Journal of Archaeological Science:*
852 *Reports*, 19, 476-490. <https://doi.org/10.1016/j.jasrep.2018.02.040>.
- 853 Maindonald, J., Braun, J., 2006. *Data analysis and graphics using R: an example-based approach (Vol. 10)*.
854 Cambridge University Press.
- 855 Martín-Fernández, J. A., Barceló-Vidal, C., Pawlowsky-Glahn, V., 2003. Dealing with zeros and missing values
856 in compositional data sets using nonparametric imputation. *Mathematical Geology*, 35, 253–278.
- 857 Mathis, F., Bodu, P., Dubreuil, O., Salomon, H., 2014. PIXE identification of the provenance of ferruginous
858 rocks used by Neanderthals, *Nucl. Instrum. Meth. B. s.* 331, 275-279. <https://doi.org/10.1016/j.nimb.2013.11.028>.

- 859 Mauran, G., 2019 *Apports méthodologiques à la caractérisation des matières colorantes: application à l'abri orné*
860 *de Leopard Cave (Erongo, Namibie)*. PhD-Dissertation, Museum national d'Histoire naturelle, Paris.
861 <https://tel.archives-ouvertes.fr/tel-03020872>
- 862 Mauran G., Lebon M., Lapauze O., Nankela M., Caron B., Détroit F., Pleurdeau D., Bahain J.J., 2020.
863 Archaeological ochres of the rock art site of Leopard Cave (Erongo, Namibia): looking for Later Stone Age socio-
864 cultural behaviours. *African Archaeological Review*, 37, 527-550. <https://doi.org/10.1007/s10437-020-09394-7>.
- 865 Mauran, G., Caron, B., Detroit, F., Nankela, A., Bahain, J. J. Pleurdeau, P., Lebon, M., 2021a. Data pretreatment
866 and multivariate analyses for ochre sourcing: Application to Leopard Cave (Erongo, Namibia), *J. Archaeol. Sci.*
867 *Rep.*, 35, 102757. <https://doi.org/10.1016/j.jasrep.2020.102757>.
- 868 Mitchell, D., Grave, P., Maccheroni, M., Gelman, E., 2012. Geochemical characterisation of north Asian glazed
869 stonewares: a comparative analysis of NAA, ICP-OES and non-destructive pXRF. *Journal of Archaeological*
870 *Science*, 39(9), 2921-2933.. <https://doi.org/10.1016/j.jas.2012.04.044>.
- 871 Moyo, S. Mphuthi, D. Cukrowska, E., Henshilwood, C. S., van Niekerk, K., Chimuka, L., 2016. Blombos cave:
872 Middle Stone Age ochre differentiation through FTIR, ICP OES, ED XRF and XRD, *Quat. Int.*, 404, 20-29.
873 <https://doi.org/10.1016/j.quaint.2015.09.041>.
- 874 Nel, P., Lynch, P. A., Laird, J. S., Casey, H. M., Goodall, L. J., Ryan, C. G., & Sloggett, R. J., 2010. Elemental
875 and mineralogical study of earth-based pigments using particle induced X-ray emission and X-ray diffraction.
876 *Nuclear Instruments and Methods in Physics Research Section A: Accelerators, Spectrometers, Detectors and*
877 *Associated Equipment*, 619(1-3), 306-310. <https://doi.org/10.1016/j.nima.2009.12.003>.
- 878 Onoratini, G., 1985. Diversité minérale et origine des matériaux colorants utilisés dès le paléolithique supérieur
879 en Provence, *Bull. Mus. Hist. Nat. (Marseille)*. 45,7-114.
- 880 Palarea-Albaladejo, J., Martín-Fernández, J. A., 2013. Values below detection limit in compositional chemical
881 data. *Analytica Chimica Acta*, 764, 32–43.
- 882 Palarea-Albaladejo, J., Martín-Fernández, J. A., Buccianti, A., 2014. Compositional methods for estimating
883 elemental concentrations below the limit of detection in practice using R. *Journal of Geochemical Exploration*,
884 141, 71–77.
- 885 Perlès, C., 1987. *Les industries lithiques taillées de Franchthi (Argolide, Grèce) I, Présentation Générale et*
886 *Industries Paléolithiques. Excavations at the Franchthi cave, Fascicle 3. Excavations at Franchthi Cave—Greece-*
887 *Indiana University Press. Bloomington. Indianapolis.*
- 888 Pichon, L., Calligaro, T., Lemasson, Q., Moignard, B., Pacheco, C., 2015. Programs for visualization, handling
889 and quantification of PIXE maps at the AGLAE facility. *Nuclear Instruments and Methods in Physics Research*
890 *Section B: Beam Interactions with Materials and Atoms*, 363, 48-54. <https://doi.org/10.1016/j.nimb.2015.08.086>.
- 891 Pichon, L., Beck, L., Walter, P., Moignard, B., Guillou, T., 2010. A new mapping acquisition and processing
892 system for simultaneous PIXE-RBS analysis with external beam. *Nuclear Instruments and Methods in Physics*
893 *Research Section B: Beam Interactions with Materials and Atoms*, 268(11-12), 2028-
894 2033. <https://doi.org/10.1016/j.nimb.2010.02.124>.
- 895 Pierce, D. E., Wright, P. J., Popelka-Filcoff, R. S., 2020. Seeing red: an analysis of archeological hematite in east
896 central Missouri. *Archaeological and Anthropological Sciences*, 12(1), 1-20. [https://doi.org/10.1007/s12520-](https://doi.org/10.1007/s12520-019-00984-4)
897 [019-00984-4](https://doi.org/10.1007/s12520-019-00984-4).
- 898 Popelka-Filcoff, R. S., Robertson, J. D., Glascock, M. D., Descantes, C., 2007. Trace element characterization of
899 ochre from geological sources. *Journal of Radioanalytical and Nuclear Chemistry*, 272(1), 17-
900 27. <https://doi.org/10.1007/s10967-006-6836-x>

- 901 Popelka-Filcoff, R. S., Miksa, E. J., Robertson, J. D., Glascock, M. D., Wallace, H., 2008. Elemental analysis
902 and characterization of ochre sources from Southern Arizona. *Journal of archaeological science*, 35(3), 752-
903 762. <https://doi.org/10.1016/j.jas.2007.05.018>.
- 904 Popelka-Filcoff, R., C. Lenehan, M. Glascock, J. Bennett, A. Stopic, J. Quinton, A. Pring, K. Walshe, 2012.
905 "Evaluation of relative comparator and k0-NAA for characterization of Aboriginal Australian ochre." *Journal of*
906 *Radioanalytical and Nuclear Chemistry* 291(1): 19-24
- 907 Popelka-Filcoff, R. S., Zipkin, A. M., 2022. The archaeometry of ochre sensu lato: A review. *Journal of*
908 *Archaeological Science*, 137, 105530. <https://doi.org/10.1016/j.jas.2021.105530>
- 909 Rifkin, R., 2015. Ethnographic and Experimental Perspectives on the Efficacy of Red Ochre as a Mosquito
910 Repellent, *S. Afr. Archaeol. Bull.*, 70, 64–75. www.jstor.org/stable/24643609.
- 911 Rifkin, R., Dayet, L., Queffelec, A., d'Errico, F., Summers, B., Lategan, M., 2015. Evaluating the
912 Photoprotective Effects of Red Ochre on Human Skin by in Vivo SPF Assessment: Implications for Human
913 Evolution, Adaptation and Dispersal, *PLoS ONE*, 10.9, e0136090. <https://doi.org/10.1371/journal.pone.0136090>.
- 914 Ripley, B., Venables, B., Bates, D. M., Hornik, K., Gebhardt, A., Firth, D., Ripley, M. B., 2013 Package 'mass'.
915 *Cran R*, 538.
- 916 Salomon, H., Vignaud, C., Coquinot, Y., Beck, L., Stringer, C., Strivay, D., d'Errico, F., 2012. Selection and
917 heating of colouring material in the Mousterian level of Es-Skhul (c. 100 000 years BP, Mount Carmel, Israel),
918 *Archaeometry*. 54(4), 698–722. <https://doi.org/10.1111/j.1475-4754.2011.00649.x>.
- 919 Salomon, H., Goemaere, E., Billard, C., Dreesen, R., Bosquet, D., Hamon, C., Jadin, I., 2016. Analyse Critique
920 du protocole de caractérisation des hématites oolithiques mis en place dans le cadre du projet collectif de
921 recherche sur L'origine des hématites oolithiques exploitées durant la Préhistoire récente entre l'Eifel (DE) et la
922 Normandie (FR). *Anthropologica et Praehistorica*, 125/2014:225–246.
- 923 Salomon, H., Chanteraud, C., de Kergommeaux, A. C., Monney, J., Pradeau, J. V., Goemaere, É., Coquinot, Y,
924 Chalmin, E., 2021. A geological collection and methodology for tracing the provenance of Palaeolithic colouring
925 materials. *Journal of lithic studies*, 8(1), 38-p. <https://doi.org/10.2218/jls.5540>.
- 926 Scadding, R., Winton, V., Brown, V., 2015. An LA-ICP-MS trace element classification of ochres in the Weld
927 Range environ, Mid West region, Western Australia, *J. Archaeol. Sci.*, 54, 300-312.
928 <https://doi.org/10.1016/j.jas.2014.11.017>.
- 929 Smith, M. A., Fankhauser, B., Jercher, M., 1998. The changing provenance of red ochre at Puritjarra rock
930 shelter, Central Australia: Late Pleistocene to present. In *Proceedings of the Prehistoric Society* 64 : 275-292.
931 Cambridge University Press.
- 932 Solé, V., Papillon, E., Cotte, M., Walter, P., Susini, J. 2007. A multiplatform code for the analysis of energy-
933 dispersive X-ray fluorescence spectra. *Spectrochim. Acta, Part B*, 62(1):63–68.
934 <https://doi.org/10.1016/j.sab.2006.12.002>.
- 935 Speakman, R. J., Little, N. C., Creel, D., Miller, M. R., Iñáñez, J. G., 2011. Sourcing ceramics with portable
936 XRF spectrometers? A comparison with INAA using Mimbres pottery from the American Southwest. *Journal of*
937 *archaeological science*, 38(12), 3483-3496. <https://doi.org/10.1016/j.jas.2011.08.011>.
- 938 Speakman, R. J., Shackley, M. S., 2013. Silo science and portable XRF in archaeology: a response to Frahm.
939 *Journal of Archaeological Science*, 40(2), 1435-1443. <https://doi.org/10.1016/j.jas.2012.09.033>.
- 940 Steenstra, E. S., Berndt, J., Klemme, S., van Westrenen, W., Heginbotham, A., Davies, G. R., 2021. Analysis of
941 the CHARM Cu-alloy reference materials using excimer ns-LA-ICP-MS: Assessment of matrix effects and
942 applicability to artefact provenancing. *Archaeometry*, 1– 16. <https://doi.org/10.1111/arcm.12729>

943 Swann, C. P., Fleming, S. J., 1990. Selective filtering in PIXE spectrometry. *Nuclear Instruments and Methods*
944 *in Physics Research Section B: Beam Interactions with Materials and Atoms*, 49(1-4), 65-69.
945 [https://doi.org/10.1016/0168-583X\(90\)90217-I](https://doi.org/10.1016/0168-583X(90)90217-I).

946 Tsolakidou, A., Kilikoglou, V., 2002. Comparative analysis of ancient ceramics by neutron activation analysis,
947 inductively coupled plasma–optical-emission spectrometry, inductively coupled plasma–mass spectrometry, and
948 X-ray fluorescence. *Analytical and bioanalytical chemistry*, 374(3), 566-572. [https://doi.org/10.1007/s00216-](https://doi.org/10.1007/s00216-002-1444-2)
949 [002-1444-2](https://doi.org/10.1007/s00216-002-1444-2).

950 Vega, E., Leroy, S., Dillmann, P., Pagès, G., Hendrickson, M., Téreygeol, F., 2019. L'analyse chimique des
951 déchets sidérurgiques sur le terrain par pXRF Un jeu d'échelle sous contraintes. in C. Benech, N. Cantin, M.-A.
952 Languille, A. Mazuy, L. Robinet, A. Zazzo (Eds.), *Instrumentation portable. Quels enjeux pour l'archéométrie?*,
953 Editions des Archives Contemporaines, Paris, pp.213-229

954 Velliky, E. C., MacDonald, B. L., Porr, M., Conard, N. J., 2021. First large-scale provenance study of pigments
955 reveals new complex behavioural patterns during the Upper Palaeolithic of south-western Germany,
956 *Archaeometry*, 63(1), 173-193. <https://doi.org/10.1111/arc.12611>.

957 Wadley, L., 2005a. Ochre Crayons or Waste Products? Replications Compared with MSA 'Crayons' from
958 Sibudu Cave, South Africa, *Before Farming*, 3, 1–12. <https://doi.org/10.3828/bfarm.2005.3.1>.

959 Wadley, L., 2005b. Putting Ochre to the Test: Replication Studies of Adhesives That May Have Been Used for
960 Hafting Tools in the Middle Stone Age, *J. Hum. Evol.* 49, 587–601.
961 <https://doi.org/10.1016/j.jhevol.2005.06.007>. Wei, T., Simko, V., Levy, M., Xie, Y., Jin, Y., Zemla, J., 2017.
962 Package 'corrplot'. *Statistician*, 56, 316-324.

963 Weigand, P., Harbottle, G., Sayre, E. V., 1977. Chapter 2 - Turquoise sources and source analysis: Mesoamerica
964 and the southwestern U.S.A. In : Earle, T.K., Ericson, J. (Eds.), *Exchange Systems in Prehistory*, Academic
965 Press, 15-34, <https://doi.org/10.1016/B978-0-12-227650-7.50008-0>.

966 Wickham, H., 2011. ggplot2. *Wiley Interdisciplinary Reviews: Computational Statistics*, 3(2), 180-185.

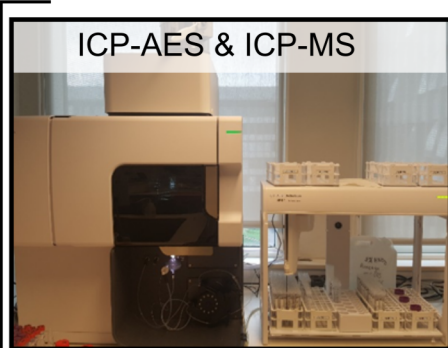
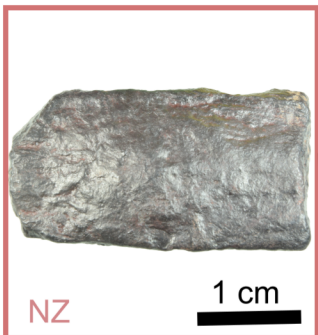
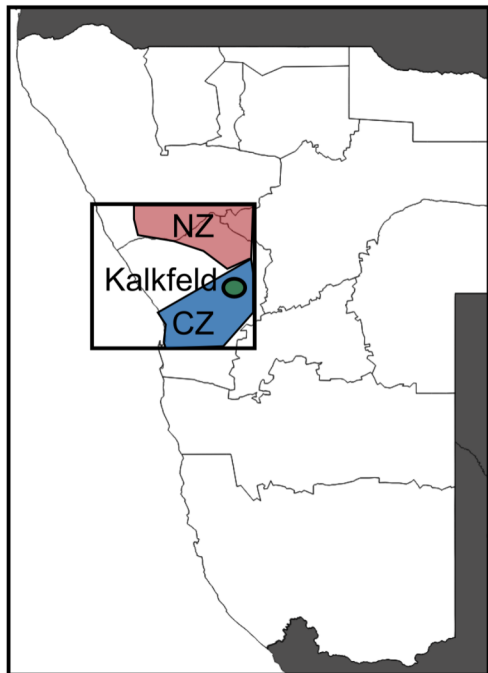
967 Yellin, J., Perlman, I., Asaro, F., Michel, H. V., Mosier, D. F., 1978. Comparison of neutron activation analysis
968 from the Lawrence Berkeley Laboratory and the Hebrew University. *Archaeometry*, 20(1), 95-100.
969 <https://doi.org/10.1111/j.1475-4754.1978.tb00219.x>.

970 Zipkin, A. M., Ambrose, S. H., Hanchar, J. M., Piccoli, P. M., Brooks, A. S., & Anthony, E. Y., 2017. Elemental
971 fingerprinting of Kenya Rift Valley ochre deposits for provenance studies of rock art and archaeological
972 pigments. *Quaternary International*, 430, 42-59. <https://doi.org/10.1016/j.quaint.2016.08.032>.

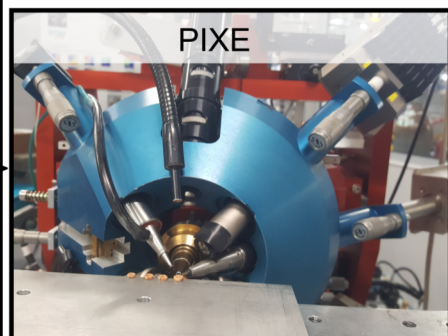
973 Zipkin, A. M., Ambrose, S. H., Lundstrom, C. C., Bartov, G., Dwyer, A., Taylor, A. H., 2020. Red Earth, Green
974 Glass, and Compositional Data: A New Procedure for Solid-State Elemental Characterization, Source
975 Discrimination, and Provenience Analysis of Ochres. *Journal of Archaeological Method and Theory*, 27(4), 930-
976 [970.https://doi.org/10.1007/s10816-020-09448-9](https://doi.org/10.1007/s10816-020-09448-9).

Proveniencing

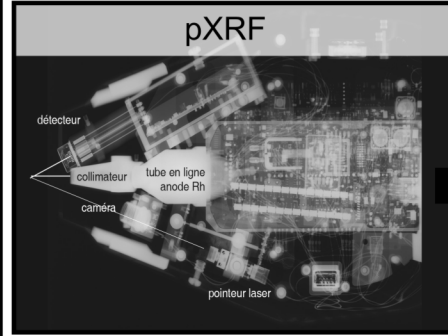
ferruginous coloring materials



Data set ICP



Data set PIXE

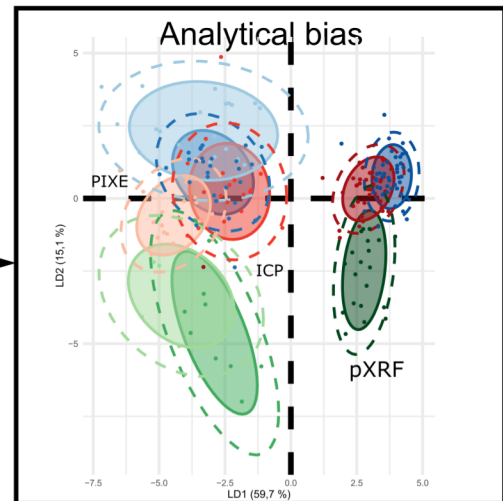


Data set pXRF

Standardization

Standardization over the 3 datasets

$$x_{ij} = \frac{C_{ij} - \bar{C}_i}{\sigma C_i}$$



Standardization of each data set separately

$$x_{ij} = \frac{C_{ij} - \bar{C}_i}{\sigma C_i}$$

